UC Berkeley
UC Berkeley Previously Published Works

Title
Impact of long-range electrostatic and dispersive interactions on theoretical predictions of adsorption and catalysis in zeolites

Permalink
https://escholarship.org/uc/item/6wz9w1q3

Authors
Mansoor, Erum
Van der Mynsbrugge, Jeroen
Head-Gordon, Martin
et al.

Publication Date
2018-08-01

DOI
10.1016/j.cattod.2018.02.007

Peer reviewed

eScholarship.org Powered by the California Digital Library
University of California

Catalysis Today 312 (2018) 51–65

Contents lists available at ScienceDirect

Catalysis Today

journal homepage: www.elsevier.com/locate/cattod

Impact of long-range electrostatic and dispersive interactions on theoretical predictions of adsorption and catalysis in zeolites

Erum Mansoor[a], Jeroen Van der Mynsbrugge[a], Martin Head-Gordon[b,c], Alexis T. Bell[a,*]

[a] Department of Chemical and Biomolecular Engineering, University of California, Berkeley, CA 94720-1462, United States
[b] Department of Chemistry, University of California, Berkeley, CA 94720-1462, United States
[c] Chemical Sciences Division, Lawrence Berkeley National Laboratory, Berkeley, CA 94720, United States

ARTICLE INFO

Keywords:
Long-range interactions
Dispersion
Electrostatics
DFT
Zeolites
QM/MM

ABSTRACT

In this paper, we review the importance of long-range zeolite framework interactions in theoretical predictions for a variety of zeolite-catalyzed processes, and we show why such interactions must be determined accurately in order to reproduce experimentally measured adsorption and activation energies. We begin with an overview of the different strategies that have been used to account for long-range coulombic and dispersive interactions of zeolite framework atoms with species adsorbed at an active site. These methods include full periodic-DFT calculations and multi-layer hybrid techniques. Electrostatic interactions are observed to have a more significant impact than dispersive interactions on the geometries of ion-pair transition states and adsorbed species. Stabilization of the TS relative to reactant complexes is also dictated by electrostatic interactions. Dispersion effects are found to significantly stabilize both transition and reactant states for adsorbed species, especially those which have dimensions that provide good fits within the zeolite pore or cavity. We also show that the relevance of particular active site configurations can be missed, if the effects of long-range interactions are neglected. As a case in point, we demonstrate that a site previously considered inactive for ethane dehydrogenation, $[GaH_2]^+$ may in fact be more active than previously thought, when the impact of long-range interactions on the predicted activation energy is taken into account. Finally, the use of hybrid quantum mechanics/molecular mechanics approaches on extended, finite zeolite clusters has emerged as an accurate, highly cost-effective, and versatile alternative towards overcoming some of the present-day limitations of periodic calculations.

1. Introduction

Zeolites are crystalline, microporous aluminosilicates that are widely used as adsorbents and catalysts for numerous industrial processes and for the abatement of automotive pollutants [1]. The framework of zeolites comprises corner-shared TO_4 (T = Si or Al) tetrahedra, which can form complex 3-dimensional networks of channels and cages of molecular dimensions (0.2–1.2 nm) [2]. Substitution of a trivalent Al atom for a tetravalent Si atom in the zeolite framework introduces a net negative charge, which must be compensated by a proton or an extra-framework cation, resulting in Brønsted or Lewis acid sites, respectively [3]. Given the very large number of zeolite structures that can be formed (over 230 framework types are recognized by the Structure Commission of the International Zeolite Association) [4], the performance of these materials as adsorbents and catalysts is dependent on their composition and structure.

In recent years, theoretical predictions based on electronic structure calculations have emerged as a powerful tool for understanding the relationships between structure and performance of zeolites at the molecular level. Experience with the use of such methods has revealed that accurate prediction of adsorption and activation energies requires a model for the zeolite framework and a suitable electronic structure method to describe the interactions of adsorbed species at the active sites, as well as the influence of long-range coulombic and dispersive interactions associated with lattice atoms far removed from the catalytically active site.

An accurate description of the long-range electronic effects of the extended lattice atoms surrounding the active site in a computationally efficient manner has been a long-standing challenge in the area of molecular modeling of zeolites [5]. Two approaches have emerged over the past two decades to account for the long-range effects of the zeolite framework; these are referred to as finite cluster and periodic-boundary techniques (See Fig. 1). It is worth noting that both of these methods often focus on a single isolated active site in a perfect crystal, while in

* Corresponding author.
E-mail address: alexbell@berkeley.edu (A.T. Bell).

https://doi.org/10.1016/j.cattod.2018.02.007
Received 22 December 2017; Received in revised form 29 January 2018; Accepted 2 February 2018
Available online 08 February 2018
0920-5861/ © 2018 Elsevier B.V. All rights reserved.

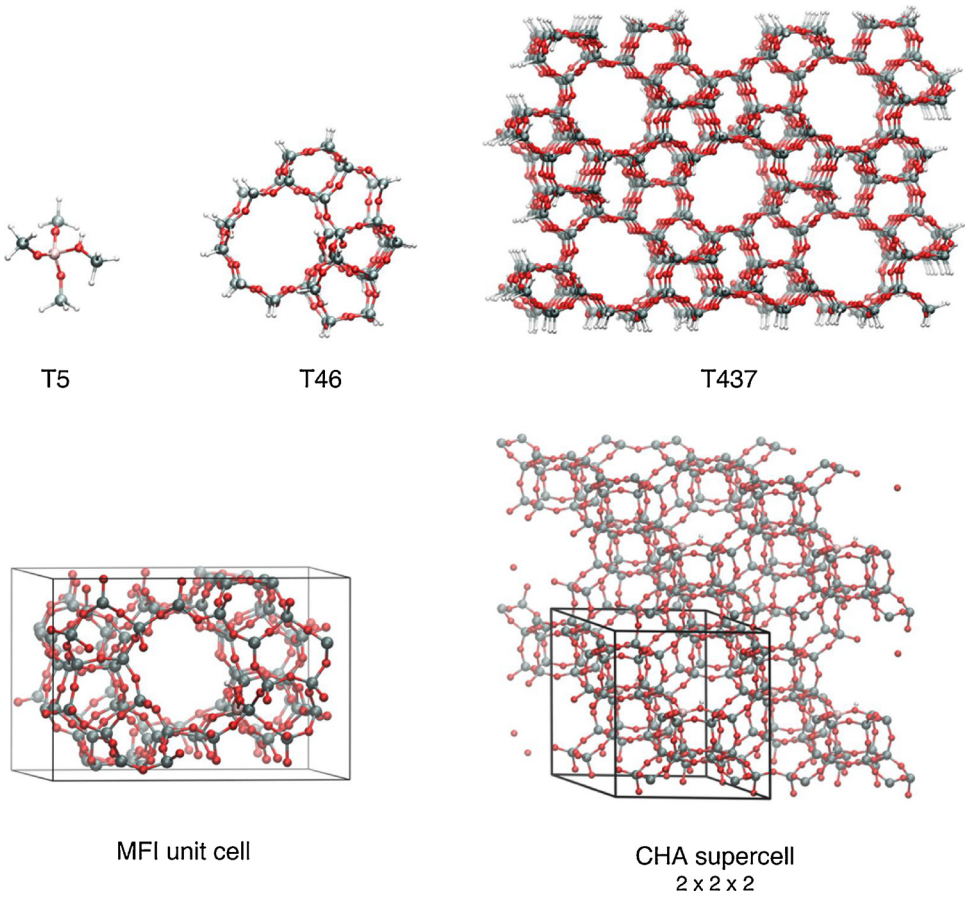

Fig. 1. Examples of finite cluster (T5, T46, T437 H-MFI fragments saturated with terminating hydrogen atoms) and periodic models (MFI unit cell and CHA $2 \times 2 \times 2$ super cell). T refers to number of tetrahedrally coordinated zeolite lattice atoms included in the model. Small cluster models are highly computationally efficient, but cannot capture shape-selective effects, nor the role of long-range electrostatics and dispersion associated with the extended zeolite lattice.

reality, the zeolite catalyst can be heterogeneous at different length and time scales [6,7]. Experimental measurements typically represent averages over local variations, defects (e.g. mesopores and terminal silanol groups) in the framework, extra-framework species and other system-specific complexities in the zeolite lattice. However, gaps between our understanding of idealized and real zeolite systems can be further minimized by judicious selection of an appropriate physical model of the active site, surrounding lattice, and associated long-range interactions for a given system [8].

In the cluster approach, the active center for adsorption or reaction and a portion of the surrounding framework are modeled by a finite zeolite fragment. To construct such a cluster model, several Si–O bonds are cleaved, which subsequently need to be saturated with terminating atoms (typically hydrogens) in order to create a chemically stable complex. Initial theoretical studies employed small clusters consisting of just three to five T-atoms representing only the active site itself. While the limited number of atoms in such a model greatly reduces the computational expense, and therefore enables the use of highly accurate electronic structure methods, the influence of the specific zeolite structure on adsorption thermodynamics and reaction kinetics owing to long-range electrostatic and dispersive interactions between the adsorbates and the framework atoms is neglected. To properly capture these effects, and to achieve agreement between calculated and experimentally measured enthalpies of molecular adsorption, a very large part of the zeolite surrounding the active site must be included. As expected, this strategy results in a rapid rise in computational cost. To offset the issue of computational expense, small clusters are often embedded in an extended hybrid model, which accounts for the long-range electrostatic and dispersive interactions of the zeolite lattice using computationally inexpensive force fields based on classical molecular mechanics or via less expensive quantum mechanical methods. Such multi-layer schemes are discussed in more detail in Section 2.2.

By contrast, in the periodic approach, one or more zeolite unit cells are simulated and infinitely repeated in all three directions by applying periodic boundary conditions. In principle, these simulations provide the most natural representation of the crystal structure and the shape and size of its pore system; however, as illustrated in Fig. 1, some industrially important zeolites exhibit large primitive unit cells (e.g., the MFI unit cell contains 288 atoms [4]), while others (e.g., CHA) require the use of super cells to properly isolate the active sites and avoid unphysical interactions between periodic images of sorbates or charged defects [9,10].

In Section 2, we briefly review commonly used theoretical tools for modeling zeolite adsorption and catalysis, with an emphasis on current implementations that account for long-range electrostatic and dispersive interactions of the zeolite framework. We discuss electronic structure methods (focusing on DFT), and their applications to zeolites in the form of full periodic DFT calculations or multi-layer hybrid schemes. Then in Sections 3–5, we illustrate the impact of long-range interactions on predictions of adsorption energies and activation barriers, as well as on conclusions reached about which sites may be active for promoting zeolite-catalyzed systems. Finally, in Section 6, we propose that the use of cost-effective hybrid quantum mechanics/molecular mechanics approaches on extended zeolite clusters is an attractive alternative to overcoming the shortcomings of periodic calculations, without compromising accuracy.

2. Brief overview of theoretical tools

2.1. Electronic structure methods

In both cluster and periodic studies, Kohn-Sham density functional theory (DFT) [11,12] is used for electronic structure calculations because of its favorable balance between accuracy and computational

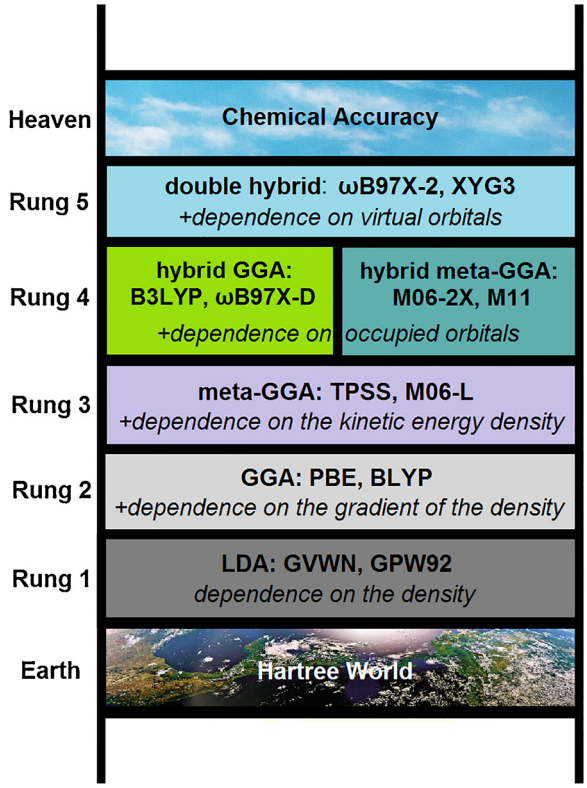

Fig. 2. Illustration of Perdew's metaphorical Jacob's Ladder, which is composed of five rungs corresponding to different levels of sophistication in DFT functionals for predicting the unknown exchange-correlation term. Each rung contains new physical information that is missing in lower rungs, leading to an improved accuracy.

cost, which is especially important for describing large systems. DFT employs a single configuration of orbitals (corresponding to non-interacting electrons) to represent the desired (interacting) electron density. The non-interacting kinetic energy, electron-nuclear attraction, and classical electron–electron repulsions are exactly treated in DFT, while non-classical exchange (X) and electron–electron correlation (C) are inexactly modeled as functionals of the electron density [13]. The choice of XC functional therefore determines the accuracy of DFT calculations, including predictions of local adsorbate-site interactions [14]. While it is a review in itself to fully discuss the range of functionals available [15–17], as well as their strengths and weaknesses, we present a short overview of the issues associated with DFT-based predictions, and their connections to modeling reactive chemistry in zeolites.

A large number of DFT functionals with different levels of sophistication has been developed. They are commonly categorized into rungs on a metaphorical Jacob's Ladder [18,19] , as illustrated in Fig. 2, according to the physical variables on which the XC functional depends. Rung 1 defines the famous local spin density approximation (LSDA), which is exact for the uniform electron gas. As the simplest XC model, the LSDA depends only on the electron density, $\rho(\mathbf{r})$, but is known to be grossly inaccurate for chemical reaction energies. Rung 2 is defined as the generalized gradient approximations (GGAs), in which the XC energy also depends on $\nabla\rho(\mathbf{r})$. GGAs are only a little more computationally demanding than the LSDA, yet are far more accurate. For this reason, GGAs are still commonly used when computational cost considerations are paramount. Widely used examples include PBE [20,21] and revPBE [22,23], which are quite often employed in periodic zeolite calculations.

However, standard GGA functionals are unable to describe dispersion forces originating from long-range electron–electron correlations, which result in attractive interactions between molecules even in the absence of permanent charges or dipole moments. Dispersive interactions are a crucial part of zeolite-adsorbate interactions, and neglecting them can cause a significant underestimation of the absolute values of adsorption enthalpies. Different approaches can be taken to remedy the lack of dispersion in DFT calculations. The simplest and most popular is the DFT-D scheme proposed by Grimme, in which an empirical damped atom–atom R^{-6} potential term is added to the standard DFT energy at negligible additional computational expense [24,25]. DFT-D methods have been used in various zeolite studies using both finite-sized clusters and periodic structures (cf. infra). Subsequent generations have expanded the availability of D-corrections to most elements in the periodic table, while carefully parameterizing the more sophisticated empirical atom–atom forms to promote transferability across a variety of chemical systems [26–28]. Widely used dispersion-corrected GGAs include the B97-D3 functional, as well as PBE-D3. With virtually zero additional computational cost, use of dispersion-corrected GGAs is nowadays standard in preference to uncorrected GGAs.

The empirical atom–atom dispersion corrections can also be replaced by higher accuracy alternatives which introduce density dependence either explicitly or implicitly into the dispersion energy expression. One example of implicit density dependence, recently proposed by Tkatchenko and Scheffler, involves a parameter-free derivation of the interatomic coefficients in the dispersion term [29]. Perhaps the most fundamental approach is the development of nonlocal correlation (NLC) models [18,30], where the dispersion energy depends simultaneously on the density at *two* different points in space, in contrast to the way in which GGAs describe the XC energy in terms of values of $\rho(\mathbf{r})$ and $\nabla\rho(\mathbf{r})$ at only one position, $\mathbf{r}$, at a time. The first example was vdW-DF [31], which was later improved to yield vdW-DF2 [32]. The semi-empirical VV10 model [33] is considerably simpler and has become very popular. VV10 has been reformulated to define the virtually equivalent rVV10 [34] model for periodic calculations. These approaches are gaining traction in practical applications [31,35,36].

The third rung of Jacob's Ladder is populated by so-called meta-GGAs (mGGAs), in which the XC energy depends on $\rho(\mathbf{r})$, $\nabla\rho(\mathbf{r})$ and $\tau(\mathbf{r})$, where the latter is the kinetic energy density, and contains second derivative information, $\nabla^2\rho(\mathbf{r})$. While the development of effective GGAs can be viewed as nearly complete, the development of viable mGGAs is still an active research area. Early mGGAs such as the TPSS [37] and revTPSS [38] functionals were not viewed as significant improvements over widely used GGAs, although M06-L [39] attracted considerable interest. More recently, there have been exciting advances in first-principles-based design of mGGAs resulting in the SCAN functional [40], and also very promising semi-empirical mGGAs such as mBEEF [41], B97M-V [42] and B97M-rV [43]. The latter two functionals include dispersion via the VV10 and rVV10 NLC functionals, respectively. Based on the exciting advances in mGGA accuracy over the past few years, it seems possible that dispersion-corrected mGGAs will steadily replace GGAs as computationally affordable workhorse functionals in the future, particularly in periodic codes.

The fourth rung of Jacob's Ladder is defined by hybrid functionals which include additional dependence on the occupied Kohn-Sham orbitals. This orbital dependence means that the exact wavefunction expression for exchange can enter the functional. Such functionals really are hybrid constructs that combine DFT with wavefunction theory, a combination that is possible in generalized Kohn-Sham theory [44]. Hybrids may be formulated as hybrid GGAs (hGGAs) or hybrid mGGAs (hmGGAs). The B3LYP functional [45,46], an hGGA that includes 20% exact Hartree Fock (HF) exchange (calculated using the HF wavefunction method [47]), is the most widely used of its type for computational studies of chemical reactions over the last two decades. Thus −for better or worse– it has become almost a default method, especially for non-specialists [48]. B3LYP also gained popularity in early studies on

zeolite systems [49]. A well-established hmGGA is M06-2X, a variant of the hybrid Minnesota 06 (M06) functional containing twice as much exact HF exchange [50,51]. M06-2X has emerged as a top performer within the M06 family for main group thermochemistry, kinetics and medium-range dispersion interactions [50,51], and has also been used in studies of zeolite systems [52,53]. It is considered amongst the most robust [54] of the dozen or so Minnesota density functionals, including M06-L.

For chemical applications, hybrids offer significant improvements in accuracy over GGAs and mGGAs. However, hybrid functionals are significantly more computationally demanding than GGAs, especially in full periodic DFT calculations [55]. Hybrids help to reduce one general problem with XC functionals, which is the so-called self-interaction error (SIE) [56]. SIE causes artificial stabilization of structures with more delocalized electron configurations such as transition states, leading to an underestimation of activation energies. SIE can be reduced by including a larger fraction of exact HF exchange (e.g. M06-2X), or by introducing range separation in the Coulomb operator such that the short-range part of the exchange is treated by DFT, while the long-range part is treated by wavefunction theory [55]. A prominent example of range separation is the ωB97 family of hGGA functionals (where the ω parameter determines the length scale on which the short-range part decays; typically $\omega \approx 0.8\,A^{-1}$) [57]. The range-separated and dispersion-corrected hybrid, ωB97X-D [58], has emerged as a good all-around functional, with promising performance across main group thermochemistry, kinetics and noncovalent interactions [59]. This functional has been used extensively in zeolite calculations (cf. infra). Recent improvements include the ωB97X-D3 variant [60], and the ωB97X-V functional [61]. The latter is actually a redesign that reduces the number of empirical parameters by 30%, and incorporates VV10 to significantly improve accuracy for non-bonded interactions.

Development of hmGGAs is an active research area where considerable progress is still occurring. One example is the very recently developed ωB97M-V functional [62], which was designed using a combinatorial approach to address the problem of minimizing the number of empirical parameters, whilst ensuring that the functional has maximal predictive power. This 12 parameter range-separated, hybrid meta-GGA functional with VV10 nonlocal correlation was found to statistically outperform 200 other functionals across roughly 5000 data points covering thermochemical reaction energies, barrier heights, noncovalent interactions, and isomerization energies [15]. Just as mGGAs may gradually supplant GGAs as the preferred local functionals, the very promising performance of ωB97M-V suggests that hmGGAs may also gradually become more widely used in the future, particularly for applications where the computational cost of exact exchange is not prohibitive.

The fifth and final rung of Jacob's Ladder permits the XC energy to depend on the empty or virtual orbitals, in addition to the occupied orbitals. Functionals of this type are often referred to as double hybrids, because not only do they include exact exchange by wavefunction theory, but they also include wavefunction-based correlation, via either second order Møller-Plesset theory, or the random phase approximation. Prominent examples include B2PLYP-D3 [63,64], XYG3 [65], ωB97X-2 [66], and DSD-PBEPBE-D3 [67]. These functionals offer higher accuracy than those from the lower rungs, but incur too high a computational cost to be amenable to routine applications to large molecules [68–70]. At present, for the many-atom systems that represent models of reactive zeolite chemistry, the double hybrids are affordable only as single point energy calculations on structures that have been optimized at lower levels of theory.

A number of the DFT functionals discussed above (with the exception of rung 5 functionals, and the most recently proposed members of rungs 3 and 4) have been used in zeolite applications, both on finite clusters and periodic models. At a practical level, clusters offer more flexibility, since a wider variety of DFT functionals, including recently developed hybrids can readily be employed [55], since fewer atoms are treated at the quantum level. Furthermore, efficient transition state search algorithms are less prevalent in periodic codes, and frequency calculations are more cumbersome – the latter are required both for verifying the nature of stationary points and for the calculation of the molecular partition function from which thermochemical quantities can be derived.

An issue specific to finite cluster calculations using atom-centered basis sets is the error caused by basis set incompleteness, i.e., the basis set superposition error (BSSE). BSSE often results in an overestimation of the interaction energy between fragments, leading to overestimated adsorption energies and underestimated activation energies relative to the gas phase. Most density functionals are parametrized to perform best at the complete basis set limit [15]. Formal BSSE corrections can be calculated using the counterpoise method [71], but this requires several additional (and for large systems relatively expensive) energy calculations. In practice, counterpoise calculations are usually avoided by using augmented polarized triple-zeta basis sets, which are near enough to the complete basis set limit for BSSE to become negligible compared to errors resulting from other approximations [15]. For certain semi-empirical approaches, e.g. Grimme's DFT-D methods and the M06 functionals, counterpoise corrections are even entirely unsuitable [15]. In the case of DFT-D, the training data for the parametrization of the D-correction terms was obtained with polarized triple zeta basis sets, and the remaining BSSE is expected to have been absorbed into the empirical potential. Grimme therefore suggested using such basis sets without counterpoise corrections, as these might lead to error over-compensation [24]. An interesting recent development is the geometric counterpoise correction (GCP) [72], which includes an atom–atom correction for BSSE, and the alternative DFT-C counterpoise correction [73] which was formulated specifically for the moderately sized def2-SVPD basis [74,75].

The use of full periodic DFT calculations [8] has very recently been recommended over other cluster methods for the cases of low silica zeolites ($Si/Al \leq 2$), where site cooperativity effects for reactant activation require explicit treatment of a large number of electrons on multiple active sites. However, full periodic DFT calculations are too computationally expensive for routine calculations when compared to other cluster-based methods [76,77], particularly when large zeolite unit cells are necessary. Furthermore, various theoretical studies report that popular GGA functionals used in periodic DFT [78,79], including PBE-D and vdW-DF yield poor predictions of physisorption energies in zeolites. As already discussed in this section, many interesting developments in the research of exchange-correlation functionals have recently emerged to solve such issues [62,80], pertaining to the treatment of dispersion effects. At present, advanced hybrid functionals (such as ωB97X-D and M06-2X, and more recent alternatives) that accurately capture heats of adsorption and reaction barriers in zeolites are not computationally tractable in full periodic DFT calculations [77]. Therefore, the inability to utilize high performance hybrid GGA functionals at reasonable computational cost for periodic DFT calculations nevertheless persists. That limitation can often be overcome by using highly cost-effective, electrostatically embedded, multi-layer hybrid approaches. In the following section, a brief overview of commonly used implementations of such approaches in the zeolite literature is presented.

2.2. Multi-layer hybrid approaches

Large zeolite models combined with recently developed DFT functionals have the potential to provide a very accurate description of adsorption and catalysis in zeolites. However, applying these methods to models of the required size becomes computationally prohibitive, especially since catalytic cycles typically contain several elementary steps, and thus require many calculations. A pragmatic solution is provided by multi-layer hybrid approaches, in which the computational cost of treating large systems is mitigated by dividing them into two or

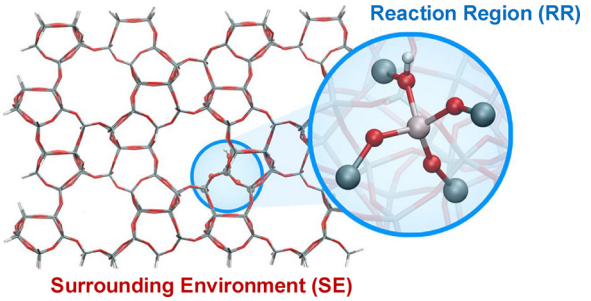

Fig. 3. Illustration of two-layer partitioning using ball-and-stick representation for the high-level "Reaction Region" containing the active site and any substrates adsorbed there, and wireframe representation for the surrounding zeolite lattice ("Surrounding Environment").

more regions, as illustrated in Fig. 3; these regions are then treated at different levels of theory. In zeolite applications, most often a relatively small portion of the system containing the active site and guest molecules (the "Reaction Region") is treated using a highly accurate electronic method, such as a modern DFT functional or a wavefunction method, while the remainder of the system (the "Surrounding Environment") is described using a computationally cheaper level of theory, such as a lower level QM method, or even classical molecular mechanics (MM).

Multi-layer hybrid approaches cover a large variety of computational schemes, depending on which methods are used to treat the Reaction and Surrounding Environment regions (RR and SE), and whether the hybrid model is set up as a subtractive or an additive scheme. In both of these schemes, the end goal is to model the RR at a high-level of theory (HL) and the SE at a low-level (LL) of theory, and this is why the RR is often referred to as the "high-level region" and the SE as the "low-level region". Commonly used subtractive and additive multi-layer hybrid approaches in the literature are briefly described below.

2.2.1. *Subtractive schemes*

The ONIOM method ("our Own N-layer Integrated molecular Orbital molecular Mechanics") was developed by Morokuma and coworkers [81]. An illustration of the subtractive scheme used in ONIOM is shown in Fig. 4; in principle, ONIOM allows any combination of high-level (HL) and low-level (LL) molecular modeling methods to be used, enabling both QM/MM and QM/QM approaches. Furthermore, the electrostatic interactions between the active site and its surrounding environment of atoms are only taken into account at the low-level of theory in ONIOM. In most cases, these electrostatic interactions are described using classical methods, which are unable to describe the behavior of electrons at the active site located in the RR.

Originally developed for biomolecular systems, a variety of ONIOM schemes has since been implemented, as reviewed in Ref. [82], including applications in studies of zeolite chemistry. In geometry optimizations and frequency calculations, the high level (HL) is typically described using a hybrid DFT functional, while the low level (LL) is treated by semi-empirical methods, e.g., AM1 [83], MNDO [84] or PM3 [85], or a molecular mechanics method, e.g., the universal force field

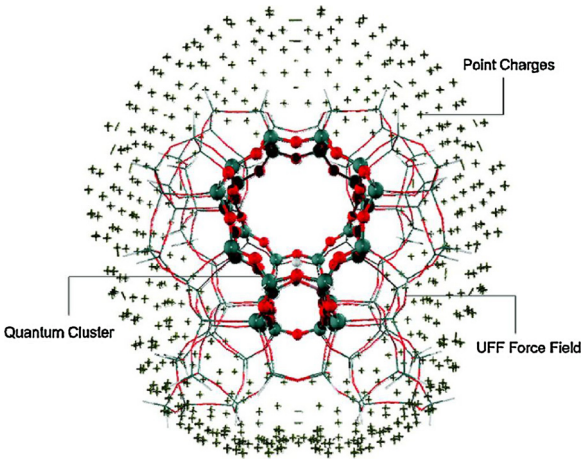

Fig. 5. Cluster with two-layer ONIOM scheme embedded in SCREEP point charges, adapted from Ref. [89] with permission. Copyright (2009) American Chemical Society. The overall model of the zeolite catalyst is represented by a T128 cluster of the H-ZSM-5 zeolite. The Reaction Region, which consists of T12 atoms, modeled using QM is illustrated with ball and stick models.

(UFF) [86]. Some authors allow the entire cluster model to relax during geometry optimizations, keeping the terminating hydrogens fixed in space to prevent the cluster from collapsing [87,88], while others only relax the RR containing the active center [52,89–91]. Following geometry optimizations at the ONIOM level, single-point energy refinements are sometimes performed on the entire cluster to minimize potential artifacts arising from the specific partitioning of the system [76,87,88,92].

Maihom et al. [89] have studied the methylation of ethene with methanol and dimethylether in H-ZSM-5 using an ONIOM scheme on a T128 cluster with a T12 QM Region treated using B3LYP or M06-2X, while the remainder of the cluster was modeled using UFF and kept frozen during geometry optimizations. These authors additionally embedded the cluster model in a set of point charges according to the Surface Charge Representation of External Embedded Potential (SCREEP) method to approximate the Madelung potential of the infinite zeolite lattice, creating an electrostatically embedded ONIOM scheme, illustrated in Fig. 5. Such electrostatically embedded variants of the ONIOM scheme have been successfully implemented to describe catalysis and adsorption in zeolites, as discussed later in more detail in Sections 3 and 4.

Other variants of subtractive multi-layer schemes with electrostatic embedding in the literature have been developed by Sierka and Sauer. One example of such methods, known as "QM-Pot", employs a quantum mechanics-interatomic potential scheme, where the force field is parametrized to DFT calculations [93]. The QM-Pot approach differs from the aforementioned ONIOM schemes in that the interatomic potential is implemented with periodic boundary conditions, and also with a polarizable ion-pair shell potential in the periodic zeolite lattice region. A review of various applications of QM-Pot calculations on the structure and reactivity of zeolites, can be found in Ref. [94]. Another example of a hybrid multi-layer approach is the QM/QM subtractive scheme (also developed by Sauer and coworkers [95]), which utilizes

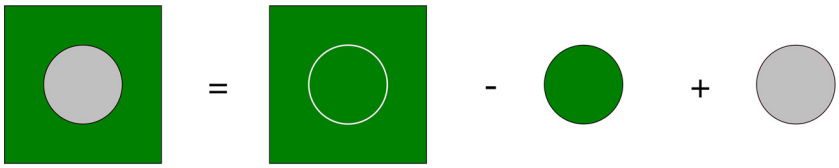

$$E_{total} = E_{(RR+SE)}^{LL} - E_{RR}^{LL} + E_{RR}^{HL}$$

Fig. 4. Schematic representation of the energy calculation in a subtractive two-layer hybrid scheme. Regions colored in grey are modeled at a high level of theory (HL), while those colored in green are at a low level of theory (LL). The region containing the active site and adsorbed substrates is referred to as the "Reaction Region" (RR), which is placed within its "Surrounding environment" (SE).

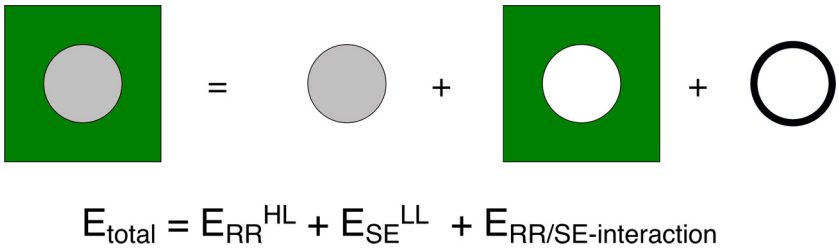

Fig. 6. Schematic representation of the energy calculation in additive two-layer hybrid scheme. Regions colored in grey are modeled at a high level of theory (HL), while those colored in green are at a low level of theory (LL). The region containing the active site and adsorbed substrates is referred to as the "Reaction Region" (RR), which is placed within its "Surrounding environment" (SE). The $E_{RR/SEInteraction}$ term, illustrated as the black ring connecting the RR and SE, is typically modeled at the lower level of theory, but can be included in the high-level calculations by means of electrostatic embedding.

wavefunction methods based on Møller–Plesset Perturbation Theory [96] at the MP2 level with Gaussian basis sets (to model the high-level RR) and plane wave periodic PBE-D2 (to represent the low-level SE of the zeolite lattice). The purpose of this extrapolative scheme is to estimate the MP2 energy of the full periodic system at the complete basis set limit. In this very recent work [95], the authors have achieved chemical accuracy of ± 2 kcal/mol for predicted ethene methylation activation barriers. Other applications of such multi-scale QM/QM schemes have been reported by Hansen and Keil [97]. Although such QM/QM schemes may be too computationally expensive for routine use, they could potentially be used to benchmark more cost-effective approaches [95].

2.2.2. Additive schemes

Hybrid multi-layer models can also be implemented using additive schemes, where the RR, to be modeled at a QM level, is surrounded by an environment that is described using more efficient MM methods. Various implementations of such QM/MM methods and their uses in different fields are reviewed in Refs. [9,98–100]. Although the end goal is similar to that of the subtractive schemes described in Section 2.2.1, the QM/MM energy in additive schemes is calculated as shown in Fig. 6. In contrast to subtractive schemes, additive schemes do not rely on MM parameters for the RR, avoiding complications when reactions occur. On the other hand, these schemes require a more careful treatment of the bonded and non-bonded interactions between atoms across the boundary between the RR and SE, represented by the $E_{RR/SEInteraction}$ term in Fig. 6.

Of particular interest to zeolite systems are the long-range electrostatic framework interactions, which are critical to providing a more complete picture of adsorbed structures in the zeolite. Consequently, mechanical embedding schemes which neglect the polarization of the QM region (containing the active site) by the Madelung potential of the zeolite lattice are ultimately limited in their ability to predict activation barriers. Zimmerman et al. [101] developed an additive QM/MM scheme for studying zeolite systems, in which a QM region typically consisting of 5 T-atoms (described using a dispersion-corrected DFT functional) is electrostatically embedded in an MM environment. The atoms in the MM region are fixed in space, and are described using classical Lennard-Jones and Coulomb force fields for which the parameters have been tuned to fit a set experimentally measured adsorption and activation energetics. The MM parameters (static point charges and Lennard Jones parameters) and link atoms properties at the QM/MM boundary were selected to reproduce the energies of T23-T44 QM clusters. This method has been recently validated to capture the heats of molecular adsorption accurately and has been successfully applied to a range of chemical systems including alkane cracking, dehydrogenation [102,103], alkene methylation[14] and other organic systems [104–106] with excellent reproduction of experimentally measured activation barriers and adsorption effects in zeolites [103]. Furthermore, the most attractive feature of this approach is its cost-effectiveness. Gomes et al. [14] have estimated that an improvement of nearly three orders of magnitude can be achieved by using a QM(T5)/MM (437) cluster in lieu of a full QM T44 region at the ωB97X-D/6-311 + + G(3df,3pd) level of theory.

In the following sections, we review selected studies that have effectively utilized the methods described above to investigate adsorptive and catalytic phenomena in zeolites. In particular, our objective is to demonstrate how the treatment of long-range electrostatics and dispersion interactions affects theoretical predictions of adsorption energies and activation barriers, as well as conclusions about the type of active sites responsible for promoting specific catalytic reactions.

3. Adsorption energy predictions

3.1. Impact of long-range electrostatics

Although early studies using T1-T4 clusters at various levels of theory [107–111] provided qualitative insights into the adsorption of alkanes and alkenes in acidic zeolites, quantitative agreement with experimentally measured adsorption energies was lacking in most cases. Various studies have subsequently demonstrated that by incorporating the long-range electrostatic effects of the zeolite lattice into their models, the gap between theoretical predictions and experimental findings can be bridged. For example, Truong and coworkers [112] investigated ethene adsorption in H-FAU using T3 cluster models at the B3LYP and MP2 levels of theory. These authors found that the prediction obtained using the T3 cluster underestimates the magnitude of the adsorption energy owing to the exclusion of long-range framework interactions; by embedding the T3 cluster at the MP2/6-31G(d,p) level of theory in a field of point charges obtained using the SCREEP method [113], they were able to predict the adsorption energy for ethene in H-FAU as −8.2 kcal/mol; this prediction which captured the effect of long-range electrostatics on the physisorbed ethene complex in H-FAU, was found to be in excellent agreement with the experimentally measured value of −9.0 kcal/mol.

The inclusion of long-range electrostatic interactions in predictions of adsorption energies has also been shown to stabilize physisorbed and chemisorbed alkene complexes (alkoxides) more than physisorbed alkanes. Marin and coworkers [114] have used periodic QM-Pot calculations treating the QM region at the MP2/TZVP level to demonstrate that apart from short-range stabilization due to the formation of the sigma bond with the framework, long-range electrostatics [115] also contribute to lowering the energies of chemisorbed alkenes, owing to the ionic nature of sigma complexes formed with the zeolite conjugate base, in the form of alkoxides. Conversely, physisorption energies for alkanes were found to be the least affected by electrostatic interactions, as adsorbed alkane complexes are relatively neutral and are, therefore, stabilized mainly by van der Waals interactions. Similar findings have also been reported by Deng et al. [116], in their investigation of the stability of various ion-pair intermediates derived from alkene interactions with protons in H-MFI. The authors showed that ionic adsorption complexes are more readily stabilized than neutral complexes by the effect of long-range framework electrostatics. These results were predicted using ONIOM calculations performed at the ONIOM(M06-2X/6-31G(d):AM1) level of theory followed by single point energy refinements at the ONIOM(MP2/6-311G(d,p):M06-2X/6-31G(d)) level.

Such long-range electrostatic stabilization of adsorbed ion-pair complexes is not limited to complexes derived from alkenes. These effects can also be observed for adsorbed complexes in other organic systems, particularly those which tend to have large dipole moments.

An example from an early study of aldol condensation chemistry is the adsorption of acetone on acidic zeolites. This complex involves a hydrogen-bonded interaction of the carbonyl group with the proton. Boefka et al. have [117] compared adsorption energies predicted using a small cluster and an electrostatically embedded ONIOM(MP2/6-311G(d,p):UFF) model. The authors predicted an adsorption energy of −33.3 kcal/mol for acetone on H-MFI, within about 2 kcal/mol of the experimentally reported adsorption energy, using the ONIOM model, while the prediction on the isolated QM cluster was −16.3 kcal/mol. This study is yet another example of the role of the electrostatic effects of the zeolite lattice in the stabilization of the adsorbate complexes with large dipole moments or strong ionic characters. In summary, capturing long-range electrostatic interactions is essential for predicting theoretical adsorption energies that agree well with experimental data.

3.2. Impact of long-range dispersion

Long-range dispersion is important for capturing the stabilization of adsorbates relative to gas phase counterparts, especially for substrates that have the "ideal fit" for the zeolite micropores. Deng and coworkers [116] have investigated the role of dispersion effects associated with the zeolite lattice. The impact of the zeolite framework on the stability of alkene-derived, carbenium-type intermediates was examined in four different zeolite clusters (T8 H-MFI, T72 H-MFI, T84 H-Y, and T80 H-BEA). The authors found that bulkier carbenium ions were selectively accommodated in the zeolite frameworks possessing larger channels or cages as their geometries could better fit the larger pores. In a later study, Deng and coworkers [118] used energy decomposition analysis (EDA) to also show that the stability of neutral adsorbates is most influenced by dispersive interactions, especially when the adsorbates tend to fit better into the micropore cavities, as illustrated in Fig. 7. Carbenium ions and alkoxide complexes were also found to be stabilized by dispersive interactions, in addition to long-range electrostatics.

As the size of adsorbates increases inside the microporous cavity, the impact of dispersive interactions is evident in the large magnitudes of the predicted adsorption energies. These effects have been reported by Boekfa, Limtrakul, and collaborators [52] who examined the adsorption of ethene, benzene, ethylbenzene, and pyridine on H-MFI. Adsorption energies predicted for ethene, benzene, ethylbenzene, and pyridine on H-MFI using electrostatically embedded ONIOM(MP2:M06-2X) calculations were found to increase as follows: −14.0, −19.8, −24.7, and −48.4 kcal/mol. This trend in adsorption energies was attributed to the increasing importance of van der Waals interactions with increasing molecular size. The authors also noted that inclusion of the Madelung potential of the extended framework stabilized the cation-anion pair comprising cationic pyridinium and anionic zeolite to a greater degree than other more neutral complexes. With the inclusion of both long-range dispersion and electrostatics taken into account, the adsorption energy of this cation-anion pair was predicted to be within 0.8 kcal/mol of the experimentally measured value.

In an independent study using periodic DFT + D, Sauer and colleagues [119] have also arrived at the same conclusion reached by the aforementioned researchers, with regards to the increasing importance of dispersion effects with increasing substrate size. In this work, dispersion alone accounted for −31.0 kcal/mol of the predicted adsorption energy for fructose in H-MFI (−49.5 kcal/mol). The authors emphasized that for large adsorbates, the inclusion of dispersion effects in the zeolite model is absolutely necessary. These effects add up considerably for large substrates, leading to very significant stabilization of adsorbed species relative to gas phase reactants.

3.3. Roles of cluster size and electronic structure methods

The choice of a high-performance density functional is critical to adequately predicting the electronic structure around the active site of the zeolite. For DFT-parametrized force fields [101], the choice of the functional becomes even more important as it ultimately affects the long-range electrostatic and dispersive interactions captured by the MM parameters. For instance, in the QM/MM scheme implemented by Zimmerman et al. the static point charges and Lennard Jones parameters were selected to reproduce the energies of full QM clusters containing T23-T44 atoms [101]. The performance of B3LYP and ωB97X-D functionals was tested in the QM region, and the latter functional was found to yield superior agreement with experimental data for adsorption energies for a range of test set molecules (including C_1–C_4 alkanes). In contrast to B3LYP, ωB97X-D captures both range-separation and dispersion effects; therefore, ωB97X-D is a more suitable choice of functional for the parametrization of long-range MM parameters, ultimately improving the accuracy of predictions made using these parameters towards capturing long-range electrostatics and dispersion effects associated with the zeolite lattice.

Along with the choice of the electronic structure method used at the QM region, another important consideration is the choice of cluster size and basis set used in QM/MM models. Gomes et al. [14] investigated the impact of DFT functionals, cluster sizes and basis sets on the accuracy of the predicted adsorption enthalpies of butene and methanol in H-MFI using electrostatically embedded QM/MM. Full QM T44 calculations were conducted to assess the impact of the functional: the B3LYP functional was found to significantly underbind the adsorbates, while ωB97X-D and M06-2X functionals were found to give better agreement with the higher level RI-MP2(FC)//T5(CBS) method [120,121], used as a reference, as shown in Fig. 8(a). At least a T150 cluster size was required to achieve convergence of adsorption enthalpies for 1-butene with the QM/MM scheme (Fig. 8(b)). It was also concluded that a near-complete triple-zeta basis set, including polarization and diffuse functions (6-311 + + G(3df,3pd)) is required to attain an accuracy of 2 kcal/mol with respect to experimentally reported adsorption enthalpies and activation barriers for ethene methylation by methanol.

Other studies have shown that the cluster size is also critical for

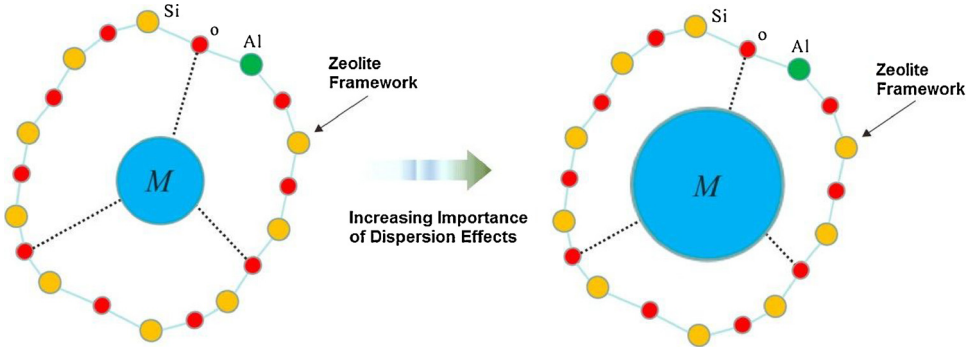

Fig. 7. Illustration of increasing substrate size in 10-ring zeolite micropore cavity leading to an ideal fit of the molecule (M). M can represent either a reactant, intermediate or TS complex in the zeolite. Adapted from Ref. [118] with permission. Copyright (2016) American Chemical Society.

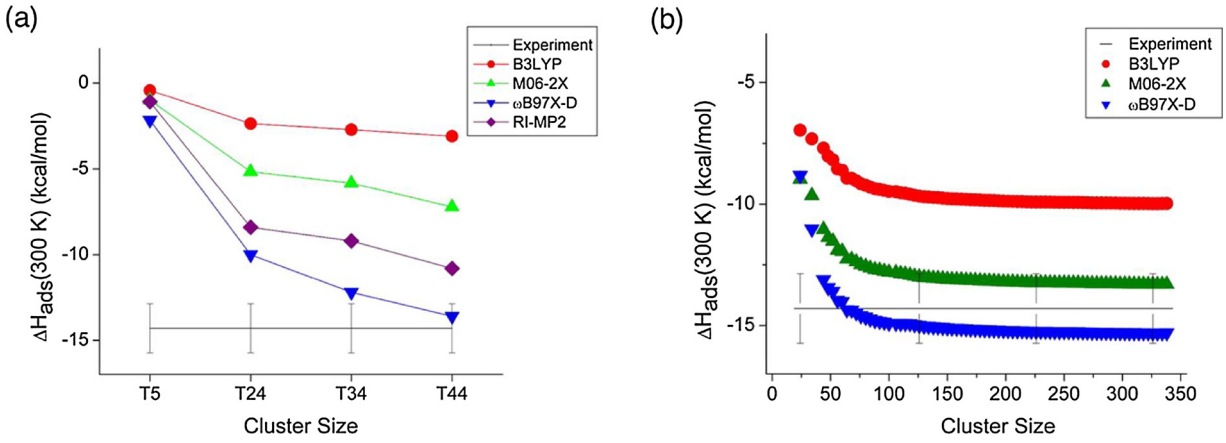

Fig. 8. Effect on predictions of adsorption enthalpy of 1-butene in H-MFI due to (a) cluster size in the full QM region and (b) functional used in the QM/MM model. Adapted from Ref. [14] with permission. Copyright (2012) American Chemical Society.

correctly parametrizing the long-range dispersion interactions in the MM region of the zeolite. Sharada et al. [102] observed that even when using a T437 cluster with a high quality functional and basis set (ωB97X-D/6-311 + + G(3df,3pd)), the chosen MM parameters had to be tuned in order to accurately capture experimental adsorption data. Significant deviations were found between experimental measurements and theoretical predictions for heats of alkane adsorption with MM parameters optimized for T23 QM clusters in earlier work [25]; the use of these parameters for the prediction of adsorption energies subsequently led to overbinding, especially for the larger alkanes. In order to bridge the aforementioned remaining gaps between theoretical and experimentally measured adsorption energies, Li et al. [103] improved the previously selected set of force-field parameters used by Sharada et al. (Parameter set P1). These parameters (P1) were modified to minimize the root-mean square (RMS) deviations of adsorption energies, which were found to systematically over bind C_1 to C_8 alkanes in siliceous MFI. The improved parametrization (P2) was obtained by scaling the characteristic energies of the Lennard-Jones potential of framework O and Si atoms so that the calculated heats of adsorption agree with those measured experimentally. Heats of adsorption determined using the improved parameters were found to agree within a RMS deviation of 1.8 kcal/mol with experimental values for two sets of test data (as opposed to 8.3 kcal/mol using P1 parameters). The test sets included both physisorption and chemisorption of guest molecules in MFI, H-MFI, and H-BEA. A comparison between the performance of parameter sets P1 and P2 is illustrated in Fig. 9. The results in these studies emphasize the importance of selecting a high-performance functional, basis set and adequate cluster size in order to adequately capture adsorption energies in zeolites.

4. Reaction barrier predictions

4.1. Impact of long-range electrostatics

Numerous studies published since the early 2000 s [122–130] have demonstrated that long-range electrostatic interactions are critical not only for accurately capturing experimentally measured activation barriers, but also for providing a complete picture of transition state structures involved in catalysis. One such seminal study on the impact of long-range electrostatics on the calculated activation barrier for alkane cracking in zeolites was conducted by Zygmunt and coworkers [122]. In this work, the impact of long-range effects of the zeolite cluster on the barrier for ethane cracking in H-MFI was investigated by varying the cluster size used to represent the MFI lattice. Transition state and stationary point energies were calculated for T5, T18, T28, T38, T46, and T58 cluster models of H-MFI, at the HF/6-31G(d) level of theory, with the atoms beyond the T5 region remaining fixed at their crystallographic positions. The authors reported that the T58 zeolite cluster provided TS stabilization on the zero point-corrected PES by approximately 15 kcal/mol relative to predictions made using the T5 cluster. It was noted that the long-range Madelung field of the zeolite crystal in the T58 cluster had a larger impact on the transition state relative to the reactant state, since the TS was more ionic in nature, owing to its larger dipole moment. This electrostatic stabilization

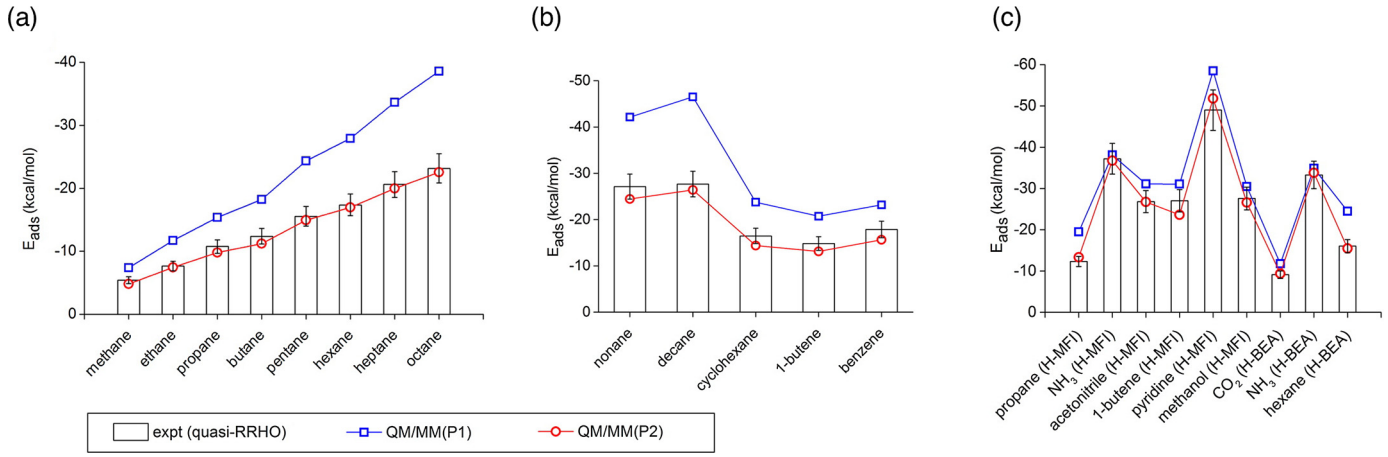

Fig. 9. Improved performance of P2 parameters for (a) training set, (b) and (c) test sets illustrating transferability to other adsorbates and zeolites. Adapted from Ref. [103] with permission. Copyright (2015) American Chemical Society. The predicted adsorption energies in (a) and (b) are calculated for guest molecules in siliceous MFI.

associated with the extended framework led to a final activation energy prediction of 54.1 kcal/mol for ethane cracking in H-MFI at the MP2(FC)/6-311 + G(3df,2p) level, which was much smaller than that found earlier for ethane cracking barriers (70–80 kcal/mol); this study was the first to point out the sensitivity of activation barrier predictions for ethane cracking to long-range electrostatic effects. The authors also reported [123] observing similar results for propane dehydrogenation, for which the barrier was stabilized by 18 kcal/mol when the dehydrogenation TS was embedded in a 64T cluster model of H-MFI. These results provided early evidence that the TS structures for the cracking of alkanes on H-MFI are especially sensitive to long-range electrostatic effects. In later studies [124–126] by Nascimento and coworkers, the dehydrogenation and cracking of isobutane over HZSM-5 were both examined at the B3LYP/6-31G(d,p) level. Activation energies predicted for T5 and T20 clusters were found to differ by up to 12 kcal/mol. It was concluded that in order to predict reliable activation energies, a final correction of about 14–16 kcal/mol was necessary to account for long-range framework electrostatics, based on T93 cluster calculations.

Other studies have shown that the importance of including the Madelung potential is not limited to accurate prediction of activation barriers but also to predicting the structure of the TS. Vollmer and Truong [127] analyzed the mechanism of hydrogen exchange of methane with H-FAU (H-Y). In this paper, the authors compared predicted activation barriers calculated for isolated and embedded T3 clusters. The latter model accounted for the long-range electrostatic potential (Madelung field) associated with the zeolite lattice using SCREEP. Single point calculations done using a Coupled Cluster wavefunction method [131] at the CCSD(T)/6-31G(d,p) level yielded barrier heights for 29.7 ± 1.2 and 32.8 ± 1.2 kcal/mol for hydrogen exchange on two different binding sites, both of which were found to be in excellent agreement with the experimentally measured value of 29.2–31.1 kcal/mol. Not only did the authors find that the bare T3 cluster predicted activation barriers in poor agreement with experimental data, but it was also inadequate for predicting the structure of the TS. The presence of long-range electrostatics in the embedded model led to the lengthening of O–H distances in the H-exchange TS by 0.10 Å and the shortening of C–H distances by 0.05 Å. Furthermore, the electrostatic potential of the zeolite lattice was observed to have a sizable impact on the total Mulliken charge distribution on the protonated methane fragment, increasing the charge from +0.21e (in the bare cluster) to +0.67e (in the embedded cluster). In this study as well, the importance of long-range electrostatic interactions on the TS structure and accuracy of predicted activation barriers was emphasized. This electrostatic stabilization effect associated with the zeolite catalyst is in principle analogous to “electric field catalysis” effects, which have very recently been emphasized in the enzyme catalysis research community [128,129]. Similar effects are experimentally observed in enzyme catalysis when a reacting molecule is placed in an environment that stabilizes the transition state’s dipole moment through electric fields, when compared to the preceding reactant complex. Fried et al. [130] have recently presented a simple model of such electrostatic catalysis effects for the ketosteroid isomerase enzyme for carbonyl bond cleavage chemistry. Here the “electric field catalysis” effect of the enzyme provides TS stabilization relative to the reactant complex by increasing the dipole moment along the C═O bond. As zeolite catalysts are often thought of as analogues to enzymes, we propose that the aforementioned model can, at least in theory, be extended to the electrostatic field effects of the zeolite lattice on TS stabilization.

4.2. Roles of long-range dispersion versus electrostatics in TS stabilization

A recent study by Janik and coworkers [132] investigated the importance of dispersive interactions on the predicted activation barriers for hydride transfer on H-MOR. As the growth of alkoxide chains has been proposed to be limited by hydride transfer between alkanes and alkoxides, the authors investigated the ability of H-MOR to catalyze the hydride transfer step as the length of the alkyl chain is increased. To this end, dispersion-corrected periodic density functional theory (DFT) calculations were used to evaluate the energetics of hydride transfer over H-MOR. The transition states for hydride transfer were found to involve carbenium ion-pair complexes. Although the inclusion of dispersion interactions was critical for capturing the reaction energetics, it was not observed to have a significant impact on the geometries or stabilities of intermediate structures along the hydride transfer reaction path, nor on the activation barriers associated with the elementary steps of formation of the hydride complex. In a recent study, Deng and coworkers [118] have independently reached similar conclusions from a Principal Component Analysis (PCA). The authors showed that when comparing different adsorbed TS and intermediate complexes on the zeolite surface, dispersion interactions, were not found to play a crucial role in improving reaction activity to the same extent as the long-range electrostatic interactions on a given PES. Dispersion effects may be negligible as they roughly cancel out between the reactant and transition state complexes in a given elementary step. Conversely, the difference in electrostatic interactions between the reactant and transition states, caused by the variation of charge properties of adsorbed species, was found to play an important role in the selective stabilization of the TS on the PES. Such an electrostatically controlled TS stabilization effect is expected to be relevant in systems where the active sites are all occupied by reactant or intermediate complexes in the reaction mechanism as opposed to being bare; in these instances, the stabilization of the TS relative to other intermediates adsorbed at the active sites is now of catalytic consequence, as opposed to TS stabilization relative to gas phase species.

Another consideration in the stabilization of a TS is how well its shape and structure is stabilized by particular micropore sizes and topologies; the importance of long-range dispersion effects becomes especially relevant here when the TS structure for a certain reaction possesses the “ideal fit” for a selected pore structure. In such special instances, the TS is selectively stabilized in the pore structure where it fits best when compared with other pore structures or zeolite topologies. An example of such selective TS stabilization effects has been observed experimentally by Iglesia and coworkers [133,134], for the carbonylation of methanol and dimethyl ether to methyl acetate, which were shown to be selectively catalyzed by zeolites containing 8-rings, such as MOR and FER. Corma and coworkers [135] subsequently performed a theoretical investigation of the activity and selectivity on protons located in 8-rings and 12-rings in H-MOR for carbonylation reactions. They noted that the predicted activation barrier for the methoxide carbonylation was 6 kcal/mol lower for protons in the 8-rings than in the 12-rings, in qualitative agreement with experimental findings. The inclusion of dispersion corrections was found to be essential to predicting this outcome. This study highlights the importance of including long-range dispersion interactions, especially for theoretical predictions of shape selective catalysis [136].

5. Theoretical predictions of active site structures

The significance of long-range framework interactions is not limited to the accurate prediction of activation barriers and adsorption energies in zeolite-catalyzed systems. The examples discussed in the previous sections have mainly focused on adsorption and reactions on Brønsted acid sites. While a great deal is already known about acidic zeolites, metal-exchanged zeolites are less well understood. Knowledge about the chemical structure of metal-exchanged active sites is a prerequisite for understanding their exceptional catalytic activity and selectivity for certain reactions. However, as detailed and complete information on the activity of various metal cation structures is not always easily accessible to experimental investigations [137], theoretical predictions of the structures and activities of various sites have emerged as an invaluable tool in this regard. Therefore, for studies involving the analysis of the activity of various sites in zeolites, the inclusion of long-range

corrections in the zeolite model can be critical. To illustrate this point, we present a case study of light alkane dehydrogenation in Ga/H-MFI, a system that has been studied extensively using small finite cluster approaches. We show that by the inclusion of long-range interactions in the zeolite model, the predicted activity of $[GaH_2]^+$ cations is much higher than previously proposed.

Light alkane dehydrogenation on Ga/H-MFI is a critical step in the activation and subsequent upgrading of light alkanes to produce alkenes and aromatics. $[GaH_2]^+$ sites have been observed experimentally in Ga/H-MFI using DRIFTS, XAFS and XANES experiments [138–140] under reaction conditions for ethane dehydrogenation. Extensive DFT calculations [141–143] carried out using small cluster models of $[GaH_2]^+$ (ranging from T3 to T22 clusters) have reported apparent activation energies for ethane dehydrogenation, ranging from 54 kcal/mol to 65 kcal/mol. The authors of these studies note however, that all of the predicted activation barriers for ethane dehydrogenation on $[GaH_2]^+$ are significantly larger than the experimentally measured activation barrier of 39 kcal/mol for Ga_2O_3/H-MFI [144].

In light of this disagreement between theoretical predictions and experiments, Joshi et al. [145] concluded that univalent $[GaH_2]^+$ must be inactive for ethane dehydrogenation and proposed that a different site [145] may be responsible for the exceptional activity of Ga/H-MFI for ethane dehydrogenation, namely $[GaH]^{2+}$. The authors conducted a very detailed mechanistic investigation of various configurations of $[GaH]^{2+}$ sites at different Al–Al pairs in the MFI framework [146]. They found that the only site for which the ethane dehydrogenation barrier was comparable to the experimental value, $E_{a,app}$ = 38.5 kcal/mol, is $[GaH]^{2+}$ associated with charge-exchanged sites involving a pair of proximate framework Al atoms located more than 0.55 nm apart. Based on the agreement between the predicted value of 38.5 kcal/mol with the experimental value, 39 kcal/mol, the authors concluded that $[GaH]^{2+}$ cations and not $[GaH_2]^+$ cations are active for ethane dehydrogenation in Ga/H-MFI.

However, none of the aforementioned studies accounted for the impact of long-range electrostatic and dispersion corrections due to the extended zeolite lattice. Consequently, the possibility that DFT-predicted activation barriers for ethane dehydrogenation on $[GaH_2]^+$ cations [141–143,145] were overestimated due to shortcomings of small cluster models used rather than due to the inherent inactivity of univalent cations was not investigated. To this end, we have assessed the impact of long-range interactions on light alkane dehydrogenation catalysis on $[GaH_2]^+$. The active site structure for $[GaH_2]^+$ was described by a T5 QM cluster, electrostatically embedded within the interior of a T432 MM cluster, as shown in Fig. 10. The QM/MM approach, reparametrized by Li et al. [103], was used to capture molecular adsorption and reaction barrier heights. Geometry optimizations and transition state searches were performed using the default algorithms implemented in Q-Chem [147]. The alkane dehydrogenation mechanism investigated was the stepwise alkyl mechanism [141], which is illustrated in Fig. 11 for ethane dehydrogenation. Note that earlier studies have predicted barriers using the zero-point corrected potential energy surface (PES) rather than the free energy surface. Therefore, the values we report in Table 1, using our QM/MM approach have also been extracted from the PES, for the sake of comparison to the results reported in these earlier papers.

The activation barrier heights predicted by QM/MM and shown in Table 1 are significantly lower than those reported previously as a consequence of the added long-range corrections in the QM/MM calculations. We further probed the individual effect of changing the functional, basis set, and cluster size, on these barrier heights. For this purpose, we focused solely on ethane dehydrogenation. The PES for this process is shown by the hollow circles and light blue-line plotted in Fig. 12. Also plotted in this figure are potential energy landscapes generated by varying the cluster size (T437 versus full QM T5), basis set (6-311++G(3df,3pd) versus 6-31G(d,p)) and functional (ωB97X-D versus B3LYP). The contribution of individual effects to the predicted barrier height for the TS3 bottleneck is shown in Table 2.

The results presented in Table 2 reveal that a barrier change of −5.0 kcal/mol for TS3 can be attributed to basis set incompleteness while that of −6.5 kcal/mol can be attributed to a change of functional. This latter difference occurs due to the added dispersion and range separation effects included in ωB97X-D, but which are neglected by B3LYP. A change in cluster size has the most significant impact, −17.6 kcal/mol, on the stabilization of TS3 due to long-range dispersion and electrostatics. This decrease in the TS3 barrier additionally includes changes in the TS geometries induced by the presence of the Madelung Potential of the zeolite, effects which were discussed in more detail in Section 4.1. We also find that the dipole moment of TS3 (relative to SI2) increases from 2.4 Debye to 3.5 Debye when going from a T5 to T437 cluster, suggesting that the stronger polarization of TS3 (when compared with SI2) is a consequence of the inclusion of the electrostatic field of the framework in the QM/MM model. Taken together, these results enable us to rationalize the substantial decrease in the predicted barrier for ethane dehydrogenation determined using QM/MM.

The remaining question is whether $[GaH_2]^+$ plays an active role in the dehydrogenation of ethane to ethene. To this end, we have carried out detailed analyses of the Gibbs free energy surfaces of various dehydrogenation mechanisms for this reaction occurring on both $[GaH_2]^+$ and $[GaH]^{2+}$ cations [148]. We find, based on an energetic

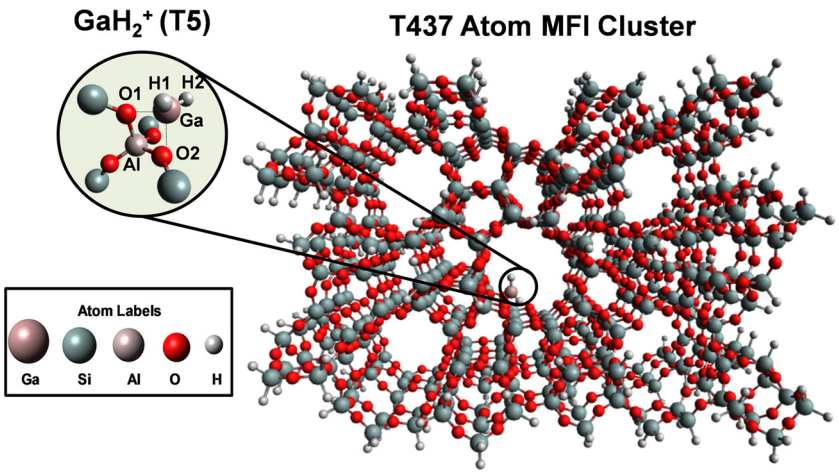

Fig. 10. View along [010] axis of T437 atom MFI structure used to model $[GaH_2]^+$ site occurring in Ga/H-MFI. The T12 site was chosen as the Al exchange location. MM parameters improved to accurately capture adsorption effects in MFI were chosen from Ref. [103]. Adapted from Ref. [148].

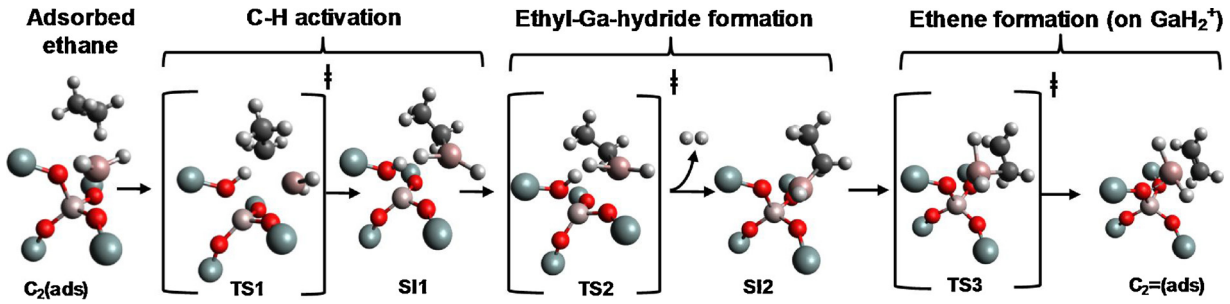

Fig. 11. Ethane dehydrogenation via Stepwise Alkyl Mechanism on GaH_2^+. Only the QM region from the QM/MM model has been displayed here to illustrate the elementary steps in this mechanism. The atom labeling scheme is the same as that in Fig. 10. SI refers to a Surface Intermediate. Adapted from Ref. [148].

Table 1
A comparison of barrier height predictions using long-range corrected QM/MM versus prior finite QM cluster predictions in the literature. Electronic energy barriers ($\Delta E^{\ddagger}$) are calculated at 0 K for the dehydrogenation of light alkanes (C_2, C_3, C_4 and iC_4) via the stepwise alkyl mechanism on $[GaH_2]^+$. The level of theory used to calculate the barriers is at ωB97X-D/6-311 + +G(3df,3pd)//ωB97X-D/6-31G(d,p).

Model Details	Pereira et al. [142]	Pidko et al. [141]	Pereira et al. [142]	QM/MM
Cluster Size	T5	T8	T22	T5(QM)/ T432(MM)
DFT Functional	B3LYP	B3LYP	B3LYP	ωB97X-D
Basis Set	LACVP(d,p)	6-31G(d,p)	LACVP(d,p)	6-311 + +G(3df,3pd)
$\Delta E^{\ddagger}_{C2}$ (kcal/mol)	65	61.7	54.0	40.1
$\Delta E^{\ddagger}_{C3}$ (kcal/mol)	64.5	–	48.0	31.2
$\Delta E^{\ddagger}_{nC4}$(kcal/mol)	57.5	–	50.5	31.3
$\Delta E^{\ddagger}_{iC4}$ (kcal/mol)	59.5	–	49.6	32.9

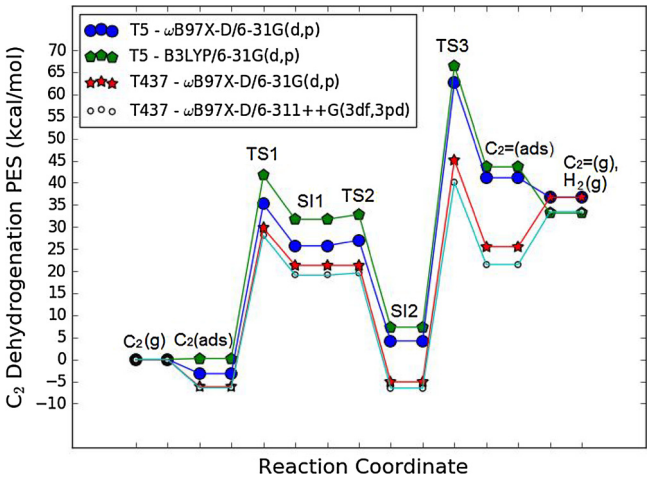

Fig. 12. Comparison of 0 K potential energy landscapes generated using QM/MM and finite QM clusters. The potential energies represented here are the zero-point corrected electronic energies for the dehydrogenation of ethane via the stepwise alkyl mechanism on $[GaH_2]^+$. SI stands for Surface Intermediate. Larger clusters significantly stabilize TS3, with smaller effects associated with the choice of basis set and functional.

span analysis reported, that $[GaH_2]^+$ can indeed compete with $[GaH]^{2+}$ sites for the dehydrogenation of ethane. This study predicts an activation enthalpy barrier of 27.5 kcal/mol, which is in very good agreement with the experimentally reported barrier of 30.5 kcal/mol for ethane dehydrogenation on well-dispersed and active Ga-exchanged sites in Ga/H-MFI, which form upon in situ reduction [144,149].

6. Summary and outlook

Quantum chemical calculations have become an increasingly powerful tool for providing insights into adsorption and catalysis in zeolite

Table 2
Effect of individual model variables (Cluster size, DFT Functional and basis set size) on predicted C_2 Dehydrogenation PES. Electronic energy barriers ($\Delta E^{\ddagger}$) at zero Kelvin are calculated using both model variables and the difference between them is reported as the barrier change.

Fixed variables	Variable in model	Change in model variable	TS3 Barrier change (kcal/mol)
T5, ωB97X-D	Basis set Size	6-31G(d,p) → 6-311 + +G(3df,3pd)	−5.0
T5, 6-31G(d,p)	DFT functional	B3LYP → ωB97X-D	−6.5
ωB97X-D, 6-31G(d,p)	Cluster size	T5 → T437	−17.6

systems. Bridging the gap between theoretical predictions and experimental observations requires the use of large zeolite models, which can be accomplished either via extended finite clusters or periodically repeated unit cells. Combined with high performance electronic structure methods, such renditions of the zeolite can capture the specific structural features of the active site, in addition to the long range electrostatic and dispersive interactions caused by the extended lattice. While periodic simulations provide the most natural representation of zeolite crystals, they are limited by high computational costs for zeolites with large unit cells, and practical drawbacks, such as the limited availability of contemporary dispersion-corrected, range-separated hybrid functionals and efficient transition state search algorithms in periodic codes. Multi-layer hybrid schemes such as ONIOM, QM/MM and QM-Pot can mitigate the high computational expense of treating large systems, and have been applied extensively to zeolites. Electrostatically embedded QM/MM schemes on extended, finite cluster models using advanced hybrid functionals such as ωB97X-D and near-complete triple zeta basis sets have emerged as an interesting alternative to periodic simulations, affording accurate predictions of adsorption energies and activation barriers at a much lower computational cost.

The work reviewed in the preceding sections highlights the importance of long-range zeolite framework interactions for predicting accurate adsorption energies and reaction barriers, and for correctly assessing the potential of specific active centers to promote catalytic processes. The inclusion of long-range electrostatic and dispersion interactions is critical for the successful reproduction of experimentally measured adsorption energies and activation barriers. We recall that large clusters, containing at least 150 T atoms, are necessary to adequately capture long-range effects on zeolite-confined adsorption and catalysis and to achieve convergence with respect to cluster size.

Long-range electrostatic interactions are observed to have the most significant impact on the geometries and stabilization of ion-pair transition states and adsorbed species in the zeolite. Consequently, mechanical embedding schemes that do not account for the polarization of the QM region by the Madelung potential of the zeolite lattice, are unable to predict intrinsic activation energies, supporting the necessity for an electrostatically embedded approach. The stabilization of

transition states relative to reactant complexes by long-range electrostatic interactions is observed to increase with the increasing ionic character of the complex. Such TS stabilization can be especially significant in the case that the reactant complexes preceding the rate-limiting TS cover all bare active sites within the zeolite. On the other hand, dispersive interactions more significantly affect the stabilization of reactant and transition state complexes relative to the gas phase, and are thus more important for predicting accurate apparent activation energies. Their importance increases for substrates that provide an ideal fit to micropore environment, i.e., when the critical diameter of the substrate and pore have similar dimensions. Dispersion effects must also be included in order to capture TS shape selectivity trends with respect to different micropore environments or zeolite topologies.

We further highlight the importance of long-range framework effects through a case study of the dehydrogenation of light alkanes on Ga/H-MFI, where we report preliminary results demonstrating that the use of a model accounting for both long-range electrostatic and dispersion effects has a very significant impact on predicted reaction barriers of up to about 17.6 kcal/mol. Our results suggest $[GaH_2]^+$ sites have been overlooked as active site candidates for light alkane dehydrogenation catalysis in previous studies, whereas, as discussed above, these sites can compete with $[GaH]^{2+}$ cations for ethane dehydrogenation.

All of the aforementioned findings may also be relevant to theoretical predictions of molecular adsorption and catalysis in other types of porous materials, for which the importance of long-range effects is already being recognized, as evidenced by very recent studies on metal-organic frameworks, porous polymers, mesoporous silicates, etc. [150–155] Furthermore, disagreement between previous theoretical and experimental values of activation or adsorption energies in other zeolite-catalyzed systems may have occurred due to an inadequate account of long-range interactions. Such systems are worth re-investigating using contemporary extended finite cluster or periodic models. The results summarized here may also potentially be relevant to the in silico design [156] of zeolite adsorbents and catalysts, where different zeolite frameworks, could be compared based whether they provide the ideal long-range electrostatic and dispersion interactions, which lead to the most effective stabilization of adsorbed substrates and TSs. In a similar vein, recent studies on electric field optimization in enzymes have emphasized on the importance of electrostatics [157] in the protein scaffolding surrounding the active site, and have even reported computational strategies to improve the efficiency of electric field catalysis in de novo designed Kemp eliminases [158]. Lastly, we note from a theoretical perspective, that Energy Decomposition Analysis (EDA) and Principal Component Analysis (PCA) [118] are promising tools with regards to deconvoluting the contributions of long-range electrostatics and dispersion in selective TS stabilization.

We would like to reiterate that the models described in this review represent an idealized version of the zeolite catalyst, focusing on a single isolated active site in a perfect crystal. The success of these approaches describing experimentally measured adsorption energies and activation barriers for elementary process is necessarily limited by the extent to which the spatial heterogeneities on different length scales in real zeolite catalysts have a negligible effect on experimental observations. Accounting for these heterogeneities in space (and time) requires integrated multi-scale modeling (and molecular dynamics) techniques. An overview of this very active field of research may be found in Refs. [159–161]

Another important consideration is the accurate prediction of entropic penalties associated with adsorbed TS complexes in microporous cavities [88]. For reasons of space, the impact of zeolite-confinement on the entropies of adsorption and activation [162] and how these properties are affected by zeolite pore structures and framework topologies have not been covered in this review. The interested reader is directed to Ref. [163,164], which discuss the challenges associated with the accurate prediction of entropies of activation. Some promising advances have been made in this area. These include advanced TS configuration sampling via uncoupled mode approximations [165], metadynamics [166], and umbrella sampling [167] approaches, to name just a few. Nonetheless, considerable challenges remain in adequately modeling entropic effects at affordable computational costs.

Acknowledgements

This work was supported by a grant from Chevron Energy Technology Company, with additional support from the Director, Office of Science, Office of Basic Energy Sciences of the U.S. Department of Energy, under Contract No. DE-AC02-05CH11231. E.M. gratefully acknowledges financial support from the Abu Dhabi National Oil Company (ADNOC) through a P.h.D. Fellowship. E.M. is also thankful to Dr. Yi-Pei Li and Neelay Phadke for engaging in interesting discussions, associated with the work presented here on Ga/H-MFI. Additionally, we are appreciative of UC Berkeley's Molecular Graphics and Computation Facility (supported by NIH S10OD023532) for providing computational resources.

References

[1] M. Guisnet, J.-P. Gilson, Zeolites for Cleaner Technologies, Imperial College Press, 2002.
[2] P. Payra, P.K. Dutta, Handbook of Zeolite Science and Technology, Marcel Dekker Inc., New York, 2003.
[3] A. Corma, Inorganic solid acids and their use in acid-catalyzed hydrocarbon reactions, Chem. Rev. 95 (1995) 559–614, http://dx.doi.org/10.1021/cr00035a006.
[4] S.C. of the I.Z. Association, Database of Zeolite Structures, Iza-Structure.org. (2017). http://www.iza-structure.org/databases/(Accessed December 4, 2017).
[5] P. Nachtigall, Applications of quantum chemical methods in zeolite science, Stud. Surf. Sci. Catal. 168 (2005) 701–736, http://dx.doi.org/10.1016/S0167-2991(07)80808-1.
[6] I.L.C. Buurmans, B.M. Weckhuysen, Heterogeneities of individual catalyst particles in space and time as monitored by spectroscopy, Nat. Chem. 4 (2012) 873–886, http://dx.doi.org/10.1038/nchem.1478.
[7] B.M. Weckhuysen, Chemical imaging of spatial heterogeneities in catalytic solids at different length and time scales, Angew. Chem. Int. Ed. 48 (2009) 4910–4943, http://dx.doi.org/10.1002/anie.200900339.
[8] E.A. Pidko, Toward the balance between the reductionist and systems approaches in computational catalysis: model versus method accuracy for the description of catalytic systems, ACS Catal. 7 (2017) 4230–4234, http://dx.doi.org/10.1021/acscatal.7b00290.
[9] A.J. O'Malley, A.J. Logsdail, A.A. Sokol, C.R.A. Catlow, Modelling metal centres, acid sites and reaction mechanisms in microporous catalysts, Faraday Discuss. 188 (2016) 235–255, http://dx.doi.org/10.1039/C6FD00010J.
[10] C. Freysoldt, J. Neugebauer, C.G. Van De Walle, Fully Ab initio finite-size corrections for charged-defect supercell calculations, Phys. Rev. Lett. 102 (2009) 1–4, http://dx.doi.org/10.1103/PhysRevLett.102.016402.
[11] P. Hohenberg, W. Kohn, Inhomogeneous electron gas, Phys. Rev. 136 (1964) B864.
[12] W. Kohn, L.J. Sham, Self-consistent equations including exchange and correlation effects, Phys. Rev. 140 (1965) A1133–A1138, http://dx.doi.org/10.1103/PhysRev.140.A1133.
[13] W. Kohn, A.D. Becke, R.G. Parr, Density functional theory of electronic structure, J. Phys. Chem. 100 (1996) 12974–12980, http://dx.doi.org/10.1021/jp960669l.
[14] J. Gomes, P.M. Zimmerman, M. Head-Gordon, A.T. Bell, Accurate prediction of hydrocarbon interactions with zeolites utilizing improved exchange-correlation functionals and QM/MM methods: benchmark calculations of adsorption enthalpies and application to ethene methylation by methanol, J. Phys. Chem. C. 116 (2012) 15406–15414, http://dx.doi.org/10.1021/jp303321s.
[15] N. Mardirossian, M. Head-Gordon, Thirty years of density functional theory in computational chemistry: an overview and extensive assessment of 200 density functionals, Mol. Phys. 115 (2017) 2315–2372, http://dx.doi.org/10.1080/00268976.2017.1333644.
[16] R. Peverati, D.G. Truhlar, Quest for a universal density functional: the accuracy of density functionals across a broad spectrum of databases in chemistry and physics, Philos, Trans. R. Soc. A Math. Phys. Eng. Sci. 372 (2014), http://dx.doi.org/10.1098/rsta.2012.0476 (20120476-20120476).
[17] H.S. Yu, S.L. Li, D.G. Truhlar, Perspective Kohn-Sham density functional theory descending a staircase, J. Chem. Phys. 145 (2016) 1–23, http://dx.doi.org/10.1063/1.4963168.
[18] J. Calbo, E. Ortí, J.C. Sancho-García, J. Aragó, The nonlocal correlation density functional VV10: a successful attempt to accurately capture noncovalent interactions, Annu. Rep. Comput. Chem. 11 (2015) 37–102, http://dx.doi.org/10.1016/bs.arcc.2015.09.002.
[19] J.P. Perdew, Jacob's ladder of density functional approximations for the exchange-correlation energy, AIP Conf. Proc. 577 (2001) 1–20, http://dx.doi.org/10.1063/

1.1390175.
[20] J.P. Perdew, K. Burke, M. Ernzerhof, Generalized gradient approximation made simple, Phys. Rev. Lett. 77 (1996) 3865–3868.
[21] J.P. Perdew, K. Burke, M. Ernzerhof, Generalized gradient approximation made simple [Phys. Rev. Lett. 77, 3865 (1996)], Phys. Rev. Lett. 78 (1997) 1396.
[22] Y. Zhang, W. Yang, Comment on generalized gradient approximation made simple, Phys. Rev. Lett. 80 (1998) 890, http://dx.doi.org/10.1103/PhysRevLett.80.890.
[23] K. Yang, J. Zheng, Y. Zhao, D.G. Truhlar, Tests of the RPBE, revPBE, τ-HCTHhyb, ωB97X-D, and MOHLYP density functional approximations and 29 others against representative databases for diverse bond energies and barrier heights in catalysis, J. Chem. Phys. 132 (2010) 164117, http://dx.doi.org/10.1063/1.3382342.
[24] S. Grimme, Accurate description of van der Waals complexes by density functional theory including empirical corrections, J. Comput. Chem. 25 (2004) 1463–1473, http://dx.doi.org/10.1002/jcc.20078.
[25] S. Grimme, J. Antony, T. Schwabe, C. Mück-Lichtenfeld, C. Muck-Lichtenfeld, Density functional theory with dispersion corrections for supramolecular structures, aggregates, and complexes of (bio)organic molecules, Org. Biomol. Chem. 5 (2007) 741–758, http://dx.doi.org/10.1039/b615319b.
[26] S. Grimme, J. Antony, S. Ehrlich, H. Krieg, A consistent and accurate ab initio parametrization of density functional dispersion correction (DFT-D) for the 94 elements H-Pu, J. Chem. Phys. 132 (2010) 154104, http://dx.doi.org/10.1063/1.3382344.
[27] J. Witte, N. Mardirossian, J.B. Neaton, M. Head-Gordon, Assessing DFT-D3 damping functions across widely used density functionals: can we do better? J. Chem. Theory Comput. 13 (2017) 2043–2052, http://dx.doi.org/10.1021/acs.jctc.7b00176.
[28] E. Caldeweyher, C. Bannwarth, S. Grimme, Extension of the D3 dispersion coefficient model, J. Chem. Phys. 147 (2017), http://dx.doi.org/10.1063/1.4993215.
[29] A. Tkatchenko, M. Scheffler, Accurate molecular van der waals interactions from ground-state electron density and free-atom reference data, Phys. Rev. Lett. 102 (2009) 73005.
[30] K. Berland, V.R. Cooper, K. Lee, E. Schröder, T. Thonhauser, P. Hyldgaard, B.I. Lundqvist, van der Waals forces in density functional theory: a review of the vdW-DF method, Rep. Prog. Phys. 78 (2015), http://dx.doi.org/10.1088/0034-4885/78/6/066501.
[31] M. Dion, H. Rydberg, E. Schröder, D.C. Langreth, B.I. Lundqvist, Van der Waals density functional for general geometries, Phys. Rev. Lett. 92 (2004) 246401, http://dx.doi.org/10.1103/PhysRevLett.92.246401.
[32] K. Lee, É.D. Murray, L. Kong, B.I. Lundqvist, D.C. Langreth, Higher-accuracy van der Waals density functional, Phys. Rev. B – Condens. Matter Mater. Phys. 82 (2010) 3–6, http://dx.doi.org/10.1103/PhysRevB.82.081101.
[33] C. Link, Nonlocal Van Der Waals Density Functional: The Simpler the Better, (2014), pp. 1–10.
[34] R. Sabatini, T. Gorni, S. De Gironcoli, Nonlocal van der Waals density functional made simple and efficient, Phys. Rev. B – Condens. Matter Mater. Phys. 87 (2013) 4–7, http://dx.doi.org/10.1103/PhysRevB.87.041108.
[35] T. Thonhauser, V.R. Cooper, S. Li, A. Puzder, P. Hyldgaard, D.C. Langreth, Van der Waals density functional: self-consistent potential and the nature of the van der Waals bond, Phys. Rev. B 76 (2007) 125112, http://dx.doi.org/10.1103/PhysRevB.76.125112.
[36] A. Gulans, M.J. Puska, R.M. Nieminen, Linear-scaling self-consistent implementation of the van der Waals density functional, Phys. Rev. B 79 (2009) 201105, http://dx.doi.org/10.1103/PhysRevB.79.201105.
[37] J. Tao, J.P. Perdew, V.N. Staroverov, G.E. Scuseria, Climbing the Density Functional Ladder: Non-Empirical Meta-Generalized Gradient Approximation Designed for Molecules and Solids, (2003), pp. 3–6, http://dx.doi.org/10.1103/PhysRevLett.91.146401.
[38] J.P. Perdew, A. Ruzsinszky, G.I. Csonka, L.A. Constantin, J. Sun, Workhorse semilocal density functional for condensed matter physics and quantum chemistry, Phys. Rev. Lett. 103 (2009) 10–13, http://dx.doi.org/10.1103/PhysRevLett.103.026403.
[39] Y. Zhao, D.G. Truhlar, A new local density functional for main-group thermochemistry, transition metal bonding, thermochemical kinetics, and noncovalent interactions, J. Chem. Phys. 125 (2006), http://dx.doi.org/10.1063/1.2370993.
[40] J. Sun, A. Ruzsinszky, J. Perdew, Strongly constrained and appropriately normed semilocal density functional, Phys. Rev. Lett. 115 (2015) 1–6, http://dx.doi.org/10.1103/PhysRevLett.115.036402.
[41] J. Wellendorff, K.T. Lundgaard, K.W. Jacobsen, T. Bligaard, MBEEF. An accurate semi-local Bayesian error estimation density functional, J. Chem. Phys. 140 (2014), http://dx.doi.org/10.1063/1.4870397.
[42] N. Mardirossian, M. Head-Gordon, Mapping the genome of meta-generalized gradient approximation density functionals: the search for B97M-V, J. Chem. Phys. 142 (2015), http://dx.doi.org/10.1063/1.4907719.
[43] N. Mardirossian, L. Ruiz Pestana, J.C. Womack, C.K. Skylaris, T. Head-Gordon, M. Head-Gordon, Use of the rVV10 nonlocal correlation functional in the B97M-V density functional: defining B97M-rV and related functionals, J. Phys. Chem. Lett. 8 (2017) 35–40, http://dx.doi.org/10.1021/acs.jpclett.6b02527.
[44] A. Seidl, A. Görling, P. Vogl, J.A. Majewski, M. Levy, Generalized Kohn-Sham schemes and the band-gap problem, Phys. Rev. B 53 (1996) 3764–3774, http://dx.doi.org/10.1103/PhysRevB.53.3764.
[45] A.D. Becke, Density-functional thermochemistry. III. The role of exact exchange, J. Chem. Phys. 98 (1993) 5648, http://dx.doi.org/10.1063/1.464913.
[46] C. Lee, W. Yang, R.G. Parr, Development of the Colle-Salvetti correlation-energy formula into a functional of the electron density, Phys. Rev. B 37 (1988) 785.
[47] D.R. Hartree, The wave mechanics of an atom with a non-Coulomb central field. Part II. Some results and discussion, Math. Proc. Camb. Philos. Soc. 24 (1928) 111, http://dx.doi.org/10.1017/S0305004100011920.
[48] H. Kruse, L. Goerigk, S. Grimme, Why the standard B3LYP/6-31G* model chemistry should not Be used in DFT calculations of molecular thermochemistry: understanding and correcting the problem, J. Org. Chem. 77 (2012) 10824–10834, http://dx.doi.org/10.1021/jo302156p.
[49] S.A. Zygmunt, An assessment of density functional methods for studying molecular adsorption in cluster models of zeolites, J. Mol. Struct. THEOCHEM. 430 (1998) 9–16, http://dx.doi.org/10.1016/S0166-1280(98)90205-6.
[50] Y. Zhao, D.G. Truhlar, Density functionals with broad applicability in chemistry, Acc. Chem. Res. 41 (2008) 157–167, http://dx.doi.org/10.1021/ar700111a.
[51] Y. Zhao, D.G. Truhlar, The M06 suite of density functionals for main group thermochemistry, thermochemical kinetics, noncovalent interactions, excited states, and transition elements: two new functionals and systematic testing of four M06-class functionals and 12 other function, Theor. Chem. Acc. Theory Comput. Model. (Theoretica Chim. Acta) 120 (2008) 215–241, http://dx.doi.org/10.1007/s00214-007-0310-x.
[52] B. Boekfa, S. Choomwattana, P. Khongpracha, J. Limtrakul, Effects of the zeolite framework on the adsorptions and hydrogen-exchange reactions of unsaturated aliphatic, aromatic, and heterocyclic compounds in ZSM-5 zeolite: a combination of perturbation theory (MP2) and a newly developed density functional theory, Langmuir 25 (2009) 12990–12999, http://dx.doi.org/10.1021/la901841w.
[53] B. Boekfa, P. Pantu, M. Probst, J. Limtrakul, Adsorption and tautomerization reaction of acetone on acidic zeolites: the confinement effect in different types of zeolites, J. Phys. Chem. C 114 (2010) 15061–15067, http://dx.doi.org/10.1021/jp1058947.
[54] N. Mardirossian, M. Head-Gordon, How accurate are the minnesota density functionals for noncovalent interactions, isomerization energies, thermochemistry, and barrier heights involving molecules composed of main-group elements? J. Chem. Theory Comput. 12 (2016) 4303–4325, http://dx.doi.org/10.1021/acs.jctc.6b00637.
[55] A.T. Bell, M. Head-Gordon, Quantum mechanical modeling of catalytic processes, Annu. Rev. Chem. Biomol. Eng. 2 (2011) 453–477, http://dx.doi.org/10.1146/annurev-chembioeng-061010-114108.
[56] A.J. Cohen, P. Mori-Sánchez, W. Yang, Challenges for density functional theory, Chem. Rev. 112 (2012) 289–320, http://dx.doi.org/10.1021/cr200107z.
[57] J.-D. Chai, M. Head-Gordon, Systematic optimization of long-range corrected hybrid density functionals, J. Chem. Phys. 128 (2008) 84106, http://dx.doi.org/10.1063/1.2834918.
[58] J.-D. Chai, M. Head-Gordon, Long-range corrected hybrid density functionals with damped atom–atom dispersion corrections, Phys. Chem. Chem. Phys. 10 (2008) 6615, http://dx.doi.org/10.1039/b810189b.
[59] L. Goerigk, S. Grimme, A thorough benchmark of density functional methods for general main group thermochemistry, kinetics, and noncovalent interactions, Phys. Chem. Chem. Phys. 13 (2011) 6670–6688, http://dx.doi.org/10.1039/c0cp02984j.
[60] Y.S. Lin, G. De Li, S.P. Mao, J. Da Chai, Long-range corrected hybrid density functionals with improved dispersion corrections, J. Chem. Theory Comput. 9 (2013) 263–272, http://dx.doi.org/10.1021/ct300715s.
[61] N. Mardirossian, M. Head-Gordon, ωB97X-V: a 10-parameter, range-separated hybrid, generalized gradient approximation density functional with nonlocal correlation, designed by a survival-of-the-fittest strategy, Phys. Chem. Chem. Phys. 16 (2014) 9904, http://dx.doi.org/10.1039/c3cp54374a.
[62] N. Mardirossian, M. Head-Gordon, ω B97M-V: a combinatorially optimized, range-separated hybrid, meta-GGA density functional with VV10 nonlocal correlation, J. Chem. Phys. 144 (2016), http://dx.doi.org/10.1063/1.4952647.
[63] S. Grimme, Semiempirical hybrid density functional with perturbative second-order correlation, J. Chem. Phys. 124 (2006), http://dx.doi.org/10.1063/1.2148954.
[64] T. Schwabe, S. Grimme, Double-hybrid density functionals with long-range dispersion corrections: higher accuracy and extended applicability, Phys. Chem. Chem. Phys. 9 (2007) 3397, http://dx.doi.org/10.1039/b704725h.
[65] Y. Zhang, X. Xu, W.A. Goddard, Doubly hybrid density functional for accurate descriptions of nonbond interactions, thermochemistry, and thermochemical kinetics, Proc. Natl. Acad. Sci. 106 (2009) 4963–4968, http://dx.doi.org/10.1073/pnas.0901093106.
[66] J.-D. Chai, M. Head-Gordon, M. Head-Gordon, Long-range corrected double-hybrid density functionals, J. Chem. Phys. 131 (2009) 174105, http://dx.doi.org/10.1063/1.3244209.
[67] S. Kozuch, J.M.L. Martin, Spin-component-scaled double hybrids: an extensive search for the best fifth-rung functionals blending DFT and perturbation theory, J. Comput. Chem. 34 (2013) 2327–2344, http://dx.doi.org/10.1002/jcc.23391.
[68] H. Eshuis, J. Bates, F. Furche, Electron correlation methods based on the random phase approximation, Theor. Chem. Acc. Theory Comput. Model. (Theoretica Chim. Acta) 131 (2012) 1–18, http://dx.doi.org/10.1007/s00214-011-1084-8.
[69] F. Furche, Molecular tests of the random phase approximation to the exchange-correlation energy functional, Phys. Rev. B 64 (2001) 195120, http://dx.doi.org/10.1103/PhysRevB.64.195120.
[70] J. Harl, G. Kresse, Accurate bulk properties from approximate many-body techniques, Phys. Rev. Lett. 103 (2009) 56401, http://dx.doi.org/10.1103/PhysRevLett.103.056401.
[71] S.F. Boys, F. Bernardi, The calculation of small molecular interactions by the differences of separate total energies. Some procedures with reduced errors, Mol. Phys. 19 (2006) 553–566, http://dx.doi.org/10.1080/00268977000101561.
[72] H. Kruse, S. Grimme, A geometrical correction for the inter- and intra-molecular basis set superposition error in Hartree-Fock and density functional theory

calculations for large systems, J. Chem. Phys. 136 (2012), http://dx.doi.org/10.1063/1.3700154.
[73] J. Witte, J.B. Neaton, M. Head-Gordon, Effective empirical corrections for basis set superposition error in the def2-SVPD basis: GCP and DFT-C, J. Chem. Phys. 146 (2017), http://dx.doi.org/10.1063/1.4986962.
[74] F. Weigend, R. Ahlrichs, Balanced basis sets of split valence, triple zeta valence and quadruple zeta valence quality for H to Rn: design and assessment of accuracy, Phys. Chem. Chem. Phys. 7 (2005) 3297–3305, http://dx.doi.org/10.1039/b508541a.
[75] D. Rappoport, F. Furche, Property-optimized Gaussian basis sets for molecular response calculations, J. Chem. Phys. 133 (2010) 0–11, http://dx.doi.org/10.1063/1.3484283.
[76] V. Van Speybroeck, K. De Wispelaere, J. Van der Mynsbrugge, M. Vandichel, K. Hemelsoet, M. Waroquier, First principle chemical kinetics in zeolites: the methanol-to-olefin process as a case study, Chem. Soc. Rev. 43 (2014) 7326–7357, http://dx.doi.org/10.1039/C4CS00146J.
[77] V. Van Speybroeck, K. Hemelsoet, L. Joos, M. Waroquier, R.G. Bell, C.R.A. Catlow, Advances in theory and their application within the field of zeolite chemistry, Chem. Soc. Rev. 44 (2015) 7044–7111, http://dx.doi.org/10.1039/C5CS00029G.
[78] L. Benco, J. Hafner, F. Hutschka, H. Toulhoat, Physisorption and chemisorption of some n-hydrocarbons at the Brønsted acid site in zeolites 12-membered ring main channels: ab initio study of the gmelinite structures, J. Phys. Chem. B 107 (2003) 9756–9762, http://dx.doi.org/10.1021/jp027625z.
[79] F. Göltl, J. Hafner, Alkane adsorption in Na-exchanged chabazite: the influence of dispersion forces, J. Chem. Phys. 134 (2011), http://dx.doi.org/10.1063/1.3549815.
[80] R.Y. Brogaard, P.G. Moses, J.K. Nørskov, Modeling van der Waals interactions in zeolites with periodic DFT: Physisorption of n-Alkanes in ZSM-22, Catal. Lett. 142 (2012) 1057–1060, http://dx.doi.org/10.1007/s10562-012-0870-9.
[81] F. Maseras, K. Morokuma, IMOMM. A new integrated ab initio + molecular mechanics geometry optimization scheme of equilibrium structures and transition states, J. Comput. Chem. 16 (1995) 1170–1179, http://dx.doi.org/10.1002/jcc.540160911.
[82] L.W. Chung, W.M.C. Sameera, R. Ramozzi, A.J. Page, M. Hatanaka, G.P. Petrova, T.V. Harris, X. Li, Z. Ke, F. Liu, H.B. Li, L. Ding, K. Morokuma, The ONIOM method and its applications, Chem. Rev. 115 (2015) 5678–5796, http://dx.doi.org/10.1021/cr5004419.
[83] M.J.S. Dewar, E.G. Zoebisch, E.F. Healy, J.J.P. Stewart, Development and use of quantum mechanical molecular models. 76. AM1: a new general purpose quantum mechanical molecular model, J. Am. Chem. Soc. 107 (1985) 3902–3909, http://dx.doi.org/10.1021/ja00299a024.
[84] M.J.S. Dewar, W. Thiel, Ground states of molecules. 38. The MNDO method. Approximations and parameters, J. Am. Chem. Soc. 99 (1977) 4899–4907.
[85] J.J.P. Stewart, Optimization of parameters for semiempirical methods II. Applications, J. Comput. Chem. 10 (1989) 221–264, http://dx.doi.org/10.1002/jcc.540100209.
[86] A.K. Rappé, C.J. Casewit, K.S. Colwell, W.A. Goddard, W.M. Skiff, UFF, a full periodic table force field for molecular mechanics and molecular dynamics simulations, J. Am. Chem. Soc. 114 (1992) 10024–10035, http://dx.doi.org/10.1021/ja00051a040.
[87] J. Van der Mynsbrugge, K. Hemelsoet, M. Vandichel, M. Waroquier, V. Van Speybroeck, Efficient approach for the computational study of alcohol and nitrile adsorption in H-ZSM-5, J. Phys. Chem. C. 116 (2012) 5499–5508, http://dx.doi.org/10.1021/jp2123828.
[88] J. Van Der Mynsbrugge, J. De Ridder, K. Hemelsoet, M. Waroquier, V. Van Speybroeck, Enthalpy and entropy barriers explain the effects of topology on the kinetics of zeolite-catalyzed reactions, Chem. – A Eur. J. 19 (2013) 11568–11576, http://dx.doi.org/10.1002/chem.201301272.
[89] T. Maihom, B. Boekfa, J. Sirijaraensre, T. Nanok, M. Probst, J. Limtrakul, Reaction mechanisms of the methylation of ethene with methanol and dimethyl ether over H-ZSM-5: an ONIOM study, J. Phys. Chem. C. 113 (2009) 6654–6662, http://dx.doi.org/10.1021/jp809746a.
[90] T. Maihom, P. Pantu, C. Tachakritikul, M. Probst, J. Limtrakul, Effect of the zeolite nanocavity on the reaction mechanism of n- hexane cracking: a density functional theory study, J. Phys. Chem. C. 114 (2010) 7850–7856, http://dx.doi.org/10.1021/jp911732p.
[91] R.E. Patet, S. Caratzoulas, D.G. Vlachos, Adsorption in zeolites using mechanically embedded ONIOM clusters, Phys. Chem. Chem. Phys. 18 (2016) 26094–26106, http://dx.doi.org/10.1039/C6CP03266D.
[92] J. Van der Mynsbrugge, M. Visur, U. Olsbye, P. Beato, M. Bjørgen, V. Van Speybroeck, S. Svelle, Methylation of benzene by methanol: single-site kinetics over H-ZSM-5 and H-beta zeolite catalysts, J. Catal. 292 (2012) 201–212, http://dx.doi.org/10.1016/j.jcat.2012.05.015.
[93] M. Sierka, A. Joachim Sauer, Structure and reactivity of silica and zeolite catalysts by a combined quantum mechanics-shell-model potential approach based on DFT, Faraday Discuss. 106 (1997) 41–62, http://dx.doi.org/10.1039/a701492i.
[94] M. Sierka, J. Sauer, Hybrid quantum mechanics/molecular mechanics methods and their application, Handb. Mater. Model. (2005) 241–258.
[95] G. Piccini, M. Alessio, J. Sauer, Ab-initio calculation of rate constants for molecule-surface reactions with chemical accuracy, Angew. Chem. – Int. Ed. 55 (2016) 5235–5237, http://dx.doi.org/10.1002/anie.201601534.
[96] C. Møller, M.S. Plesset, Note on an approximation treatment for many-electron systems, Phys. Rev. 46 (1934) 618–622, http://dx.doi.org/10.1103/PhysRev.46.618.
[97] N. Hansen, F.J. Keil, Multiscale approaches for modeling hydrocarbon conversion reactions in zeolites, Chemie-Ingenieur-Technik 85 (2013) 413–419, http://dx.doi.org/10.1002/cite.201200201.
[98] M.W. Van Der Kamp, A.J. Mulholland, Combined quantum mechanics/molecular mechanics (QM/MM) methods in computational enzymology, Biochemistry 52 (2013) 2708–2728, http://dx.doi.org/10.1021/bi400215w.
[99] H. Lin, D.G. Truhlar, QM/MM. What have we learned, where are we, and where do we go from here? Theor. Chem. Acc. 117 (2007) 185–199, http://dx.doi.org/10.1007/s00214-006-0143-z.
[100] R.A. Friesner, V. Guallar, Ab initio quantum chemical and mixed quantum mechanics/molecular mechanics (QM/MM) methods for studying enzymatic catalysis, Annu. Rev. Phys. Chem. 56 (2005) 389–427, http://dx.doi.org/10.1146/annurev.physchem.55.091602.094410.
[101] P.M. Zimmerman, M. Head-Gordon, A.T. Bell, Selection and validation of charge and lennard-jones parameters for QM/MM simulations of hydrocarbon interactions with zeolites, J. Chem. Theory Comput. 7 (2011) 1695–1703, http://dx.doi.org/10.1021/ct2001655.
[102] S. Mallikarjun Sharada, P.M. Zimmerman, A.T. Bell, M. Head-Gordon, Insights into the kinetics of cracking and dehydrogenation reactions of light alkanes in H-MFI, J. Phys. Chem. C 117 (2013) 12600–12611, http://dx.doi.org/10.1021/jp402506m.
[103] Y.-P. Li, J. Gomes, S. Mallikarjun Sharada, A.T. Bell, M. Head-Gordon, Improved force-Field parameters for QM/MM simulations of the energies of adsorption for molecules in zeolites and a free rotor correction to the rigid rotor harmonic oscillator model for adsorption enthalpies, J. Phys. Chem. C 119 (2015) 1840–1850, http://dx.doi.org/10.1021/jp509921r.
[104] Y.P. Li, M. Head-Gordon, A.T. Bell, Theoretical study of 4-(hydroxymethyl)benzoic acid synthesis from ethylene and 5-(hydroxymethyl)furoic acid catalyzed by Sn-BEA, ACS Catal. 6 (2016) 5052–5061, http://dx.doi.org/10.1021/acscatal.6b01160.
[105] Y.P. Li, M. Head-Gordon, A.T. Bell, Computational study of p -xylene synthesis from ethylene and 2, 5-dimethylfuran catalyzed by H-BEA, J. Phys. Chem. C 118 (2014) 22090–22095, http://dx.doi.org/10.1021/jp506664c.
[106] Y.P. Li, M. Head-Gordon, A.T. Bell, Analysis of the reaction mechanism and catalytic activity of metal-substituted beta zeolite for the isomerization of glucose to fructose, ACS Catal. 4 (2014) 1537–1545, http://dx.doi.org/10.1021/cs401054f.
[107] V.B. Kazansky, I.N. Senchenya, Quantum chemical study of the electronic structure and geometry of surface alkoxy groups as probable active intermediates of heterogeneous acidic catalysts: what are the adsorbed carbenium ions? J. Catal. 119 (1989) 108–120, http://dx.doi.org/10.1016/0021-9517(89)90139-5.
[108] E.M. Evleth, E. Kassab, H. Jessri, M. Allavena, L. Montero, L.R. Sierra, Calculation of the reaction of ethylene, propene, and acetylene on zeolite models, J. Phys. Chem. 100 (1996) 11368–11374 http://www.scopus.com/inward/record.url?eid=2-s2.0-00001016478&partnerID=tZOtx3y1.
[109] P.E. Sinclair, A. De Vries, P. Sherwood, C.R.A. Catlow, R.A. van Santen, Quantum-chemical studies of alkene chemisorption in chabazite: a comparison of cluster and embedded-cluster models, J. Chem. Soc. Faraday Trans. 94 (1998) 3401–3408, http://dx.doi.org/10.1039/A805616A.
[110] A.M. Rigby, M.V. Frash, Ab initio calculations on the mechanisms of hydrocarbon conversion in zeolites: skeletal isomerisation and olefin chemisorption, J. Mol. Catal. A Chem. 126 (1997) 61–72, http://dx.doi.org/10.1016/S1381-1169(97)00095-2.
[111] V.B. Kazansky, M.V. Frash, R.A. Van Santen, Quantum chemical study of the isobutane cracking on zeolites, Appl. Catal. A Gen. 146 (1996) 225–247, http://dx.doi.org/10.1016/0926-860X(96)00060-9.
[112] J. Limtrakul, T. Nanok, S. Jungsuttiwong, P. Khongpracha, T.N. Truong, Adsorption of unsaturated hydrocarbons on zeolites: the effects of the zeolite framework on adsorption properties of ethylene, Chem. Phys. Lett. 349 (2001) 161–166, http://dx.doi.org/10.1016/S0009-2614(01)01108-3.
[113] E.V. Stefanovich, T.N. Truong, A simple method for incorporating madelung field effects into ab initio embedded cluster calculations of crystals and macromolecules, J. Phys. Chem. B 102 (1998) 3018–3022, http://dx.doi.org/10.1021/jp9802580.
[114] R.A. Schoonheydt, B.M. Weckhuysen, Editorial highlight molecules in confined spaces, Phys. Chem. Chem. Phys. 11 (2009) 2794, http://dx.doi.org/10.1039/b905015a.
[115] B.A. De Moor, M. Sierka, J. Sauer, G.B. Marin, Physisorption and chemisorption of hydrocarbons in H-FAU using QM-pot (MP2//B3LYP) calculations, 11796, J. Phys. Chem C 112 (2008) 11796–11812.
[116] H. Fang, A. Zheng, J. Xu, S. Li, Y. Chu, L. Chen, F. Deng, Theoretical investigation of the effects of the zeolite framework on the stability of carbenium ions, J. Phys. Chem. C 115 (2011) 7429–7439, http://dx.doi.org/10.1021/jp1097316.
[117] B. Boefka, J. Sirijareansre, P. Pantu, J. Limtrakul, A quantum chemical study of the interaction of carbonyls with H-ZSM-5 zeolite, Recent Adv. Sci. Technol. Zeolites Relat. Mater. Pts A–C 154 (2004) 1582–1588.
[118] B. Song, Y. Chu, G. Li, J. Wang, A.-Y. Lo, A. Zheng, F. Deng, Origin of zeolite confinement revisited by energy decomposition analysis, J. Phys. Chem. C. 120 (2016) 27349–27363, http://dx.doi.org/10.1021/acs.jpcc.6b09059.
[119] L. Cheng, L.A. Curtiss, R.S. Assary, J. Greeley, T. Kerber, J. Sauer, Adsorption and diffusion of fructose in zeolite HZSM-5: selection of models and methods for computational studies, J. Phys. Chem. C 115 (2011) 21785–21790, http://dx.doi.org/10.1021/jp2062018.
[120] A.M. Burow, M. Sierka, F. Mohamed, Resolution of identity approximation for the Coulomb term in molecular and periodic systems, J. Chem. Phys. 131 (2009), http://dx.doi.org/10.1063/1.3267858.
[121] R.P. Hosteny, Ab initio study of the π-electron states of trans-butadiene, J. Chem. Phys. 62 (1975) 4764–4779, http://dx.doi.org/10.1063/1.430426.
[122] S.A. Zygmunt, L.A. Curtiss, P. Zapol, L.E. Iton, Ab initio and density functional

study of the activation barrier for ethane cracking in cluster models of zeolite H-ZSM-5, J. Phys. Chem. B 104 (2000) 1944–1949, http://dx.doi.org/10.1021/jp993194h.
[123] S.A. Zygmunt, L.A. Curtiss, Quantum-chemical studies of molecular reactivity in nanoporous materials, Comput. Mater. Chem. Methods Appl. (2005) 191–245, http://dx.doi.org/10.1007/1-4020-2117-8_5.
[124] I. Milas, M.A.C. Nascimento, The dehydrogenation and cracking reactions of isobutane over the ZSM-5 zeolite, Chem. Phys. Lett. 373 (2003) 379–384, http://dx.doi.org/10.1016/S0009-2614(03)00611-0.
[125] I. Milas, M.A.C. Nascimento, A density-functional study of the dehydrogenation reaction of isobutane over zeolites, Chem. Phys. Lett. 338 (2001) 67–73, http://dx.doi.org/10.1016/S0009-2614(01)00227-5.
[126] E.A. Furtado, I. Milas, J.O. Melam De Albuquerque Lins, M.A. Chaer Nascimento, The dehydrogenation reaction of light alkanes catalyzed by zeolites, Phys. Status Solidi Appl. Res. 187 (2001) 275–288, http://dx.doi.org/10.1002/1521-396X(200109)187:1<275:AID-PSSA275>3.0.CO;2-9.
[127] J.M. Vollmer, T.N. Truong, Mechanisms of hydrogen exchange of methane with H-Zeolite Y: an ab initio embedded cluster study, J. Phys. Chem. B 104 (2000) 6308–6312, http://dx.doi.org/10.1021/jp0008445.
[128] A. Warshel, M. Levitt, Theoretical studies of enzymic reactions: dielectric, electrostatic and steric stabilization of the carbonium ion in the reaction of lysozyme, J. Mol. Biol. 103 (1976) 227–249, http://dx.doi.org/10.1016/0022-2836(76)90311-9.
[129] S.D. Fried, S.G. Boxer, Electric Fields, Ann. Enzyme Catalysis, Rev. Biochem. 86 (2017) 387–415, http://dx.doi.org/10.1146/annurev-biochem.
[130] S.D. Fried, S. Bagchi, S.G. Boxer, Extreme electric fields power catalysis in the active site of ketosteroid isomerase, Science 80 (346) (2014) 1510–1514, http://dx.doi.org/10.1126/science.1259802.
[131] G.D. Purvis, R.J. Bartlett, A full coupled-cluster singles and doubles model: the inclusion of disconnected triples, J. Chem. Phys. 76 (1982) 1910–1918, http://dx.doi.org/10.1063/1.443164.
[132] G.M. Mullen, M.J. Janik, Density functional theory study of alkane-alkoxide hydride transfer in zeolites, ACS Catal. 1 (2011) 105–115, http://dx.doi.org/10.1021/cs1000619.
[133] P. Cheung, A. Bhan, G.J. Sunley, E. Iglesia, Selective carbonylation of dimethyl ether to methyl acetate catalyzed by acidic zeolites, Angew. Chem. – Int. Ed. 45 (2006) 1617–1620, http://dx.doi.org/10.1002/anie.200503898.
[134] A. Bhan, E. Iglesia, A link between reactivity and local structure in acid catalysis on zeolites, Acc. Chem. Res. 41 (2008) 559–567, http://dx.doi.org/10.1021/ar700181t.
[135] M. Boronat, C. Martínez, A. Corma, Mechanistic differences between methanol and dimethyl ether carbonylation in side pockets and large channels of mordenite, Phys. Chem. Chem. Phys. 13 (2011) 2603, http://dx.doi.org/10.1039/c0cp01996h.
[136] C.B. Khouw, M.E. Davis, Selectivity in Catalysis, (1993), http://dx.doi.org/10.1021/bk-1993-0517.ch014.
[137] G. Centi, B. Wichterlová, A.T. Bell, N.A.T.O.S.A. Division, Catalysis by Unique Metal Ion Structures in Solid Matrices: From Science to Application, Springer, Netherlands, 2001.
[138] G.D. Meitzner, E. Iglesia, J.E. Baumgartner, E.S. Huang, The chemical state of gallium in working alkane dehydrocyclodimerization catalysts. In situ gallium K-edge X-ray absorption spectroscopy, J. Catal. 140 (1993) 209–225, http://dx.doi.org/10.1006/jcat.1993.1079.
[139] V.B. Kazansky, I.R. Subbotina, N. Rane, R.A. Van Santen, E.J.M. Hensen, On two alternative mechanisms of ethane activation over ZSM-5 zeolite modified by Zn2+ and Ga1+ cations, Phys. Chem. Chem. Phys. (2005) 3088–3092.
[140] V.B. Kazansky, I.R. Subbotina, R.A. Van Santen, E.J.M. Hensen, DRIFTS study of the chemical state of modifying gallium ions in reduced Ga/ZSM-5 prepared by impregnation. I. Observation of gallium hydrides and application of CO adsorption as molecular probe for reduced gallium ions, J. Catal. 227 (2004) 263–269, http://dx.doi.org/10.1016/j.jcat.2004.07.021.
[141] E.A. Pidko, V.B. Kazansky, E.J.M. Hensen, R.A. van Santen, A comprehensive density functional theory study of ethane dehydrogenation over reduced extra-framework gallium species in ZSM-5 zeolite, J. Catal. 240 (2006) 73–84, http://dx.doi.org/10.1016/j.jcat.2006.03.011.
[142] M.S. Pereira, A.M. da Silva, M.A.C. Nascimento, Effect of the zeolite cavity on the mechanism of dehydrogenation of light alkanes over gallium-containing zeolites, J. Phys. Chem. C (2011) 10104–10113, http://dx.doi.org/10.1021/jp201107x.
[143] M.V. Frash, R.A. Van Santen, Activation of small alkanes in Ga-exchanged zeolites: a quantum chemical study of ethane dehydrogenation, J. Phys. Chem. A 104 (2000) 2468–2475, http://dx.doi.org/10.1021/jp993414r.
[144] J. Bandiera, Y. Ben Taârit, Ethane conversion: kinetic evidence for the competition of consecutive steps for the same active centre, Appl. Catal. A Gen. 152 (1997) 43–51, http://dx.doi.org/10.1016/S0926-860X(96)00345-6.
[145] Y.V. Joshi, K.T. Thomson, The roles of gallium hydride and Brønsted acidity in light alkane dehydrogenation mechanisms using Ga-exchanged HZSM-5 catalysts: a DFT pathway analysis, Catal. Today 105 (2005) 106–121, http://dx.doi.org/10.1016/j.cattod.2005.04.017.
[146] Y.V. Joshi, K.T. Thomson, High ethane dehydrogenation activity of [GaH]2+ Al pair sites in Ga/H-[Al]ZSM-5: a DFT thermochemical analysis of the catalytic sites under reaction conditions, J. Catal. 246 (2007) 249–265, http://dx.doi.org/10.1016/j.jcat.2006.11.032.
[147] Y. Shao, L.F. Molnar, Y. Jung, J. Kussmann, C. Ochsenfeld, et al., Advances in methods and algorithms in a modern quantum chemistry program package, Phys. Chem. Chem. Phys. 8 (2006) 3172–3191, http://dx.doi.org/10.1039/B517914A.
[148] E. Mansoor, M. Head-Gordon, A.T. Bell, Computational Modeling of the Nature and Role of Ga Species for Light Alkane Dehydrogenation Catalyzed by Ga/H-MFI, (2018), pp. 1–47, http://dx.doi.org/10.1021/acscatal.7b04295 Submitted.
[149] A. Bhan, W. Nicholas Delgass, Propane aromatization over HZSM-5 and Ga/HZSM-5 catalysts, Catal. Rev. 50 (2008) 19–151, http://dx.doi.org/10.1080/01614940701804745.
[150] H. Fang, P. Kamakoti, J. Zang, S. Cundy, C. Paur, P.I. Ravikovitch, D.S. Sholl, Prediction of CO 2 adsorption properties in zeolites using force fields derived from periodic dispersion-corrected DFT calculations, J. Phys. Chem. C 116 (2012) 10692–10701, http://dx.doi.org/10.1021/jp302433b.
[151] I. Erucar, T.A. Manz, S. Keskin, Effects of electrostatic interactions on gas adsorption and permeability of MOF membranes, Mol. Simul. 40 (2014) 557–570, http://dx.doi.org/10.1080/08927022.2013.829219.
[152] W.-Y. Gao, T. Pham, K.A. Forrest, B. Space, L. Wojtas, Y.-S. Chen, S. Ma, The local electric field favours more than exposed nitrogen atoms on CO 2 capture: a case study on the rht −type MOF platform, Chem. Commun. 51 (2015) 9636–9639, http://dx.doi.org/10.1039/C5CC02573G.
[153] M.M. Deshmukh, M. Ohba, S. Kitagawa, S. Sakaki, Absorption of CO2 and CS2 into the Hofmann-type porous coordination polymer: electrostatic versus dispersion interactions, J. Am. Chem. Soc. 135 (2013) 4840–4849, http://dx.doi.org/10.1021/ja400537f.
[154] S. Kwon, H.J. Kwon, J. Il Choi, K.C. Kim, J.G. Seo, J.E. Park, S.J. You, E.D. Park, S.S. Jang, H.C. Lee, Enhanced selectivity for CO 2 adsorption on mesoporous silica with alkali metal halide due to electrostatic field: a molecular simulation approach, ACS Appl. Mater. Interfaces 9 (2017) 31683–31690, http://dx.doi.org/10.1021/acsami.7b04508.
[155] R.H. French, V.A. Parsegian, R. Podgornik, R.F. Rajter, A. Jagota, J. Luo, D. Asthagiri, M.K. Chaudhury, Y.M. Chiang, S. Granick, S. Kalinin, M. Kardar, R. Kjellander, D.C. Langreth, J. Lewis, S. Lustig, D. Wesolowski, J.S. Wettlaufer, W.Y. Ching, M. Finnis, F. Houlihan, O.A. Von Lilienfeld, C.J. Van Oss, T. Zemb, Long range interactions in nanoscale science, Rev. Mod. Phys. 82 (2010) 1887–1944, http://dx.doi.org/10.1103/RevModPhys.82.1887.
[156] B. Smit, T.L.M. Maesen, Towards a molecular understanding of shape selectivity, Nature 451 (2008) 671–678, http://dx.doi.org/10.1038/nature06552.
[157] A. Bhowmick, S.C. Sharma, T. Head-Gordon, The importance of the Scaffold for de Novo Enzymes: a case study with Kemp eliminase, J. Am. Chem. Soc. 139 (2017) 5793–5800, http://dx.doi.org/10.1021/jacs.6b12265.
[158] V. Vaissier, S.C. Sharma, K. Schaettle, T. Zhang, T. Head-Gordon, Computational optimization of electric fields for improving catalysis of a designed Kemp eliminase, ACS Catal. 8 (2018) 219–227, http://dx.doi.org/10.1021/acscatal.7b03151.
[159] S. Raimondeau, D. Vlachos, Recent developments on multiscale, hierarchical modeling of chemical reactors, Chem. Eng. J. 90 (2002) 3–23, http://dx.doi.org/10.1016/S1385-8947(02)00065-7.
[160] N. López, N. Almora-Barrios, G. Carchini, P. Błoński, L. Bellarosa, R. García-Muelas, G. Novell-Leruth, M. García-Mota, State-of-the-art and challenges in theoretical simulations of heterogeneous catalysis at the microscopic level, Catal. Sci. Technol. 2 (2012) 2405, http://dx.doi.org/10.1039/c2cy20384g.
[161] B. Kirchner, J. Vrabec (Eds.), Multiscale Molecular Methods in Applied Chemistry, Springer Berlin Heidelberg, Berlin, Heidelberg, 2012, , http://dx.doi.org/10.1007/978-3-642-24968-6.
[162] J. Van der Mynsbrugge, A. Janda, S. Mallikarjun Sharada, L.-C. Lin, V. Van Speybroeck, M. Head-Gordon, A.T. Bell, Theoretical analysis of the influence of pore geometry on monomolecular cracking and dehydrogenation of n -butane in Brønsted acidic zeolites, ACS Catal. 7 (2017) 2685–2697, http://dx.doi.org/10.1021/acscatal.6b03646.
[163] K. De Wispelaere, L. Vanduyfhuys, V. Van Speybroeck, Chapter 6–entropy contributions to transition state modeling, Model. Simul. Sci. Micro- Meso-Porous Mater. (2018) 189–228, http://dx.doi.org/10.1016/B978-0-12-805057-6.00006-5.
[164] J. Van der Mynsbrugge, A. Janda, L.-C. Lin, V. Van Speybroeck, M. Head-Gordon, A.T. Bell, Understanding Brønsted-acid catalyzed monomolecular reactions of alkanes in zeolite pores by combining insights from experiment and theory, ChemPhysChem (2017), http://dx.doi.org/10.1002/cphc.201701084.
[165] Y.-P. Li, A.T. Bell, M. Head-Gordon, Thermodynamics of anharmonic systems: uncoupled mode approximations for molecules, J. Chem. Theory Comput. 12 (2016) 2861–2870, http://dx.doi.org/10.1021/acs.jctc.5b01177.
[166] J. Gomes, M. Head-gordon, A.T. Bell, Reaction dynamics of zeolite-catalyzed alkene methylation by methanol, J. Phys. Chem. C 118 (2014) 21409–21419, http://dx.doi.org/10.1021/jp502804q.
[167] B. Ensing, A. Laio, M. Parrinello, M.L. Klein, A recipe for the computation of the free energy barrier and the lowest free energy path of concerted reactions, J. Phys. Chem. B 109 (2005) 6676–6687, http://dx.doi.org/10.1021/jp045571i.